GEOLOGY AND TECTONICS OF THE THEMIS REGIO-LAVINIA PLANITIA-ALPHA REGIO-LADA TERRA AREA, VENUS: RESULTS FROM ARECIBO IMAGE DATA

D. A. SENSKE,[1] D. B. CAMPBELL,[2] J. W. HEAD,[1] P. C. FISHER,[1] A. A. HINE,[3] A. deCHARON,[1] S. L. FRANK,[1] S. T. KEDDIE,[1] K. M. ROBERTS,[1] E. R. STOFAN,[4] J. C. AUBELE,[1] L. S. CRUMPLER,[1] and N. STACY[2]

[1]*Department of Geological Sciences, Brown University, Providence, RI, U.S.A.*, [2]*National Astronomy and Ionosphere Center, Cornell University, Ithaca, NY, U.S.A.*, [3]*National Astronomy and Ionosphere Center, Arecibo Observatory, Arecibo, PR, U.S.A. and* [4]*Jet Propulsion Laboratory, Pasadena, CA, U.S.A.*

(Received 22 March, 1991)

Abstract. New radar images obtained from the Arecibo Observatory (resolution 1.5–4.0 km) for portions of the southern hemisphere of Venus show that: the upland of Phoebe Regio contains the southern extension of Devana Chasma, a rift zone extending 4200 km south from Theia Mons and interpreted as a zone of extension; Alpha Regio, the only large region of tessera within the imaged area, is similar to tessera mapped elsewhere on the planet and covers a smaller percentage of the surface than that observed in the northern high latitudes; the upland made of Ushas, Innini and Hathor Montes consists of three distinct volcanic constructs; Themis Regio is mapped as an ovoid chain of radar-bright arcuate single and double ring structures, edifices and bright lineaments. This area is interpreted as a region of mantle upwelling and on the basis of apparent split and separated features, a zone of localized faulting and extension. Linear zones of deformation in Lavinia Planitia are characterized by lineament belts that are often locally elevated, are similar to ridge belts mapped in the northern high latitudes and are interpreted to be characterized mainly by compression; radar-bright lava complexes within Lavinia Planitia are unique to this part of the planet and are interpreted to represent areas of eruption of high volumes of extremely fluid lava; the upland of Lada Terra is bound to the north by a linear deformation zone interpreted as extensional, is characterized by large ovoids and coronae, is interpreted to be associated with an area of mantle upwelling, and is in contrast to the northern high latitude highland of Ishtar Terra. Regions of plains in the southern hemisphere cover about 78% of the mapped area and are interpreted to be volcanic in origin. Located within the area imaged (10–78° S) are 52 craters interpreted to be of impact origin ranging from 8 to 157 km in diameter. On the basis of an overall crater density of 0.94 craters/10^6 km^2, it is determined that the age of this part of the Venus surface is similar to the 0.3 to 1.0 billion year age calculated for the equatorial region and northern high latitudes. The geologic characteristics of the portion of the Venus southern hemisphere imaged by Arecibo are generally similar to those mapped elsewhere on the planet. This part of the planet is characterized by widespread volcanic plains, large volcanic edifices, and zones of linear belt deformation. The southern hemisphere of Venus differs from northern high latitudes in that tessera makes up only a small percentage of the surface area and the ovoid chain in Themis Regio is unique to this part of the planet. On the basis of the analysis presented here, the southern hemisphere of Venus is interpreted to be characterized by regions of mantle upwelling on a variety of scales (ovoids, region made up of Ushas, Innini and Hathor Montes), upwelling and extension (Themis Regio) and localized compression (lineament belts in Lavinia Planitia).

1. Introduction and Data Acquisition

During the summer of 1988, observations of Venus were made using the 12.6 cm wavelength radar facility at Arecibo, Puerto Rico. Among the data obtained were

Earth, Moon, and Planets **55**: 97–161, 1991.

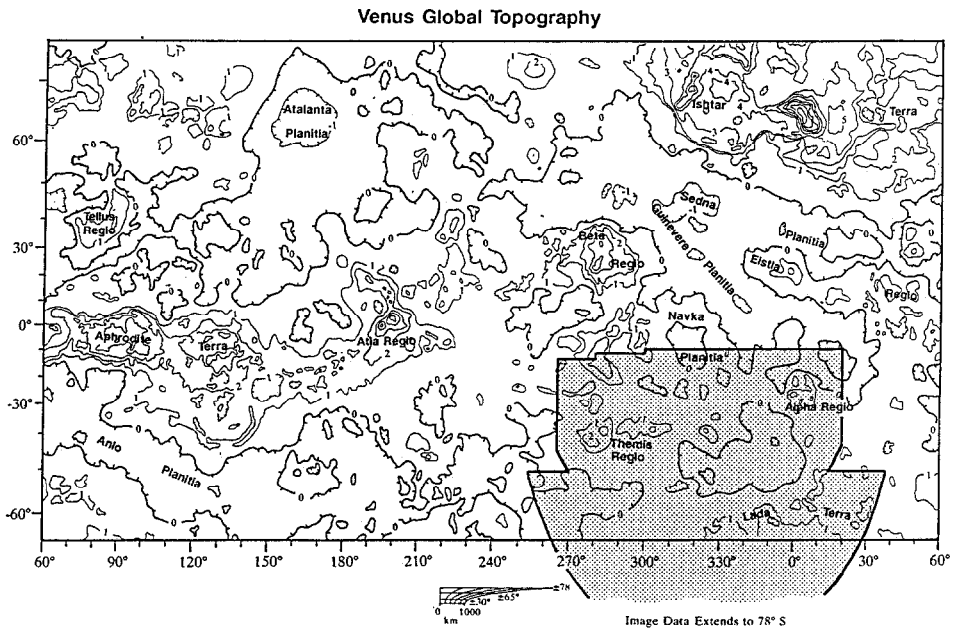

Fig. 1. Venus global topography from Pioneer Venus altimetry data contoured at 1 km intervals. The shaded region corresponds to the part of the southern hemisphere imaged from the Arecibo Observatory. The data extends from 10° S to 78° S and has a resolution from 1.5 to 4.0 km (Campbell *et al.*, 1991). The analysis presented here covers a portion of this data set extending from 10° S to 66° S and is shown of Figure 2.

images of about 55.6×10^6 km^2 of the southern hemisphere extending to 78° S with resolutions between 1.5 and 4 km (Figure 1). Data were obtained with a circularly polarized transmitted signal and the results reported here are based on images derived from the expected (i.e., single-scatter) sense of received circular polarization. The incidence angles at which the areas described here were viewed (Figure 2a) vary from about 10° to 70°. The signal-to-noise ratio for the images decreases with increasing incidence angle due to the decrease in backscatter cross-section and increased atmospheric absorption. In forming the images of the area discussed in this report (Figure 2b), twenty-five 'looks' (estimates of the backscatter cross-section) were averaged for the region from 10° to 66° S and sixteen looks were averaged from 51° to 78° S (Figures 1, 2a, b). A description of several features in this data set is found in Campbell *et al.* (1991).

The data cover several major terrains revealed by Pioneer Venus altimetry (Pettengill *et al.*, 1980; Masursky *et al.*, 1980) including the southern part of Phoebe Regio, Alpha Regio, Themis Regio and the northern part of Lada Terra. In addition, a number of planitiae (southern Navka and Guinevere, Lavinia and Helen), as well as several montes (Ushas, Innini and Hathor) are seen (Figure 2c). We describe here in detail the major geographic, geologic and tectonic features observed, discuss their similarity to features observed in other parts of Venus,

develop preliminary interpretations on the nature and relationships of the observed features and assess the age of this part of the planet on the basis of the characteristics and distribution of craters of probable impact origin. The MAGELLAN mission is scheduled to acquire high resolution image and altimetry data of the region north of about 75° S during its nominal mission (September, 1990 to May, 1991) (Saunders, *et al.*, 1990). The data and interpretations in this paper provide a synthesis and framework for the understanding of the nature of major features and processes in this region. In addition, this synthesis has raised numerous questions about the detailed nature and origin of parts of the surface and provides a basis on which to focus questions for the analysis and interpretation of the high resolution data acquired from MAGELLAN. Finally, it is well known that radar viewing geometry (look direction and incidence angle) has a strong influence on the detection and successful interpretation of the full range of surface features (MacDonald, 1980; Ford, 1980). MAGELLAN will view the surface in an E–W direction and map at incidence angles in the 15° to 40° range in this region, directions and angles that are complementary to this Arecibo data set. Together the two data sets will provide synergistic information about the nature and origin of surface features. In this paper, we first begin with a general description and synthesis of regional topography, geology and structure, proceed to detailed analyses of specific areas and features, discuss the major geologic processes, and then conclude by comparing this region to other areas of the planet.

2. General Topographic, Geologic and Tectonic Maps of the Venus Southern Hemisphere

2.1. Topographic characteristics and trends

The Themis Regio-Alpha Regio-Lada Terra portion of Venus lies south of the equatorial highlands (Phillips *et al.*, 1981), a nearly globe-encircling linear upland stretching from Western Eistla Regio eastward through Aphrodite Terra, Atla Regio, Asteria Regio and ending at Beta Regio (Figure 1). The equatorial highlands are oriented at about 21° to the equator. Topographic and geologic analyses have shown that the equatorial highlands are characterized by rifting and extension (Schaber, 1982) and that parts of the region (Aphrodite Terra) may be the site of crustal spreading (Head and Crumpler, 1987). A variety of terrain types, units and structures have been mapped in the equatorial highlands from the Pioneer Venus (PV) imaging data (Senske, 1990), the two most prominent being the tectonic junctions at Beta Regio and Atla Regio. The equatorial highlands are generally flanked by lowlands and planitiae from Western Eistla Regio eastward to Atla Regio. From Atla Regio eastward, the flanking topography becomes diffuse due to several factors including: (1) the presence of the Atla-Themis tectonic zone (Schaber, 1982) and (2) the presence of the Beta-Phoebe uplands and the generally north-south trends of the rift zones there (McGill, 1981; Stofan

et al., 1989). Both of these major disruptions extend into the mapped area (Figure 1). There is a 2000–3000 km break in the otherwise generally continuous high topography of the equatorial highlands between Beta and Western Eistla, where Guinevere Planitia intervenes and extends southward into the northern part of the mapped area. Finally, Lada Terra, the uplands of the southern high latitudes previously unseen in high resolution images, are partly covered in the new data (Figure 1 and 2c).

Geologic mapping: methods, unit description and unit characterization

A variety of volcanic and tectonic features have been observed on the surface of Venus in both the northern high latitudes and the equatorial region (Barsukov *et al.*, 1986; Sukhanov *et al.*, 1989; Campbell *et al.*, 1989; Senske 1990). The new high-resolution radar images have allowed us to classify and map features and units in that part of the planet and compare their distribution and possible modes of origin with features in other parts of Venus. These data are also used to examine the geology of the Venus southern hemisphere and make comparisons with the northern high latitudes observed by Veneras 15/16 (Barsukov *et al.*, 1986) and the equatorial region (Campbell *et al.*, 1989; Senske, 1990; Senske *et al.*, 1991).

In compiling the geologic and tectonic maps (Figures 2d, e), four factors must be taken into consideration: (1) variable incidence angle, (2) variable illumination azimuth, (3) north-south ambiguity and (4) variation in signal to noise ratio. Radar image data analyzed here covers a region extending from 10° S to 66° S and longitudes of 265° to 20° E. Incidence angles for these data range from 10° to 70° (Figure 2a). Radar return at low incidence angles and generally low latitudes (less than 25°) is primarily sensitive to variations in topographic slope, while incidence angles at latitudes greater than 25° are sensitive to variations in surface roughness at the 12.6 cm wavelength of the radar. Although the incidence angle generally scales with latitude in a N–S direction from the subradar point, the planet is being illuminated in rings and thus the incidence angle varies as shown in Figure 2a. This geometry means that the detection of features will vary as a function of latitude and longitude with, for example, small domes being detected preferentially at low incidence angles and latitudes (Aubele, 1990) and linear zones of high roughness (faults and scarps) being preferentially detected at high latitudes.

The illumination geometry illustrated in Figure 2a also indicates the variation in illumination azimuth. It is well known that the detection of linear elements is enhanced when they are oriented normal to the illumination azimuth (MacDonald, 1980) and care must be exercised in interpreting and mapping linear elements in geologic (Figure 2d) and tectonic (Figure 2e) maps in specific areas, and in comparing units and features from one place to another. Therefore, it is important to view the geologic and tectonic maps, and the geologic sketch maps, together with Figure 2a illustrating the illumination geometry. The north-south ambiguity (Evans and Hagfors, 1964) results in some of the brighter areas in the northern hemisphere (e.g., Beta and Phoebe Regio) being reflected as mirror images in the southern

image. These factors must be taken into account in distinguishing variations in radar backscatter during unit mapping. We have utilized Arecibo mirror images of the northern regions, as well as Pioneer Venus images and roughness and reflectivity maps and Arecibo images obtained under different viewing geometries, to account for the N–S radar ambiguity during mapping. Signal to noise ratio decreases as a function of latitude due to the increased path-length through the atmosphere and decreased backscatter cross section. Thus, care should be exercised in interpreting the texture of units and comparing them as a function of incidence angle and latitude. Finally, map units are often defined as radar-bright and radar-dark, which refers to the relative degree of radar backscatter detected. Since this is radar wavelength-dependent (and thus system-dependent), differences between the units defined here and those mapped with other radar systems will provide important information on the variations in the roughness characteristics of the surfaces as a function of scale.

On the basis of variations in radar backscatter, patterns in backscatter and characteristic structures of the surface, the images have been subdivided into six major radar geologic units (Table I). Basic principles of geologic mapping and stratigraphic unit nomenclature (ACSN, 1961), modified for remote sensing (Head *et al.*, 1978) and planetary applications (Wilhelms, 1970; 1972; Saunders and Mutch, 1980; Sukhanov *et al.*, 1989), have been utilized. These units are generally the same as those mapped in the equatorial region (Senske *et al.*, 1991).

The most abundant unit mapped in the southern hemisphere is **plains**, characterized by broad expanses of distinctive surface textures which generally lie in lower areas and often have lava flows or apparent volcanic source regions within them. Plains units have been divided into sub-classes on the basis of either homogeneous or heterogeneous texture seen at scales of tens to hundreds of km. *Homogeneous plains* include predominantly radar *dark plains* and *bright plains*. *Heterogeneous plains* are made up of *mottled plains*, *stippled plains*, and *digitate plains*. The distribution of plains units is not uniform. Regions of *dark plains* are found in western Lavinia Planitia, in Lada Terra, in the zone between Phoebe Regio and Themis Regio and to the east of Alpha Regio. A prong of dark plains extends to the north between the region made up of Ushas, Innini and Hathor Montes and Alpha Regio. Similar characteristics of this unit are seen at incidence angles ranging from 20° to 70°, suggesting that this unit is smooth at centimeter and longer wavelengths. Regions of *bright plains* are more patchy and are found primarily in the area between longitudes of 335° and 10° in southernmost Guinevere Planitia adjacent to Alpha Regio and eastern Lavinia Planitia. The texture of this unit suggests the presence of features that are rough at radar wavelengths.

The *mottled plains* unit is found primarily between latitudes of 10° and 40° S and longitudes 305° and 15° in southern Navka and northern Lavinia Planitiae. The mottled appearance of this unit is due to the presence of both radar-bright lobate features interpreted to be lava flows and volcanic domes. This large region of mottled plains forms the southern extension of a mottled plains unit mapped

TABLE I

Geologic units in the Venus southern hemisphere

Unit	Characteristics
Plains	
Homogeneous plains	
Dark plains	Radar-dark homogeneous texture; smooth at 12.6 cm radar wavelength; little indication of individual lava flows or systems of lava flows; found predominantly in topographically low regions
Bright plains	Predominantly relatively radar-bright homogeneous texture with some interspersed radar-dark material. Slightly mottled on the scale of 100's of km; little indication of individual lava flows; occurs in topographically low areas. Local indications of overlapping bright and dark plains units; These areas are transitional to mottled plains.
Heterogeneous plains	
Mottled plains	Characterized by polygonal components of radar-bright and radar-dark material on the scale of 100's of km; located in regions of low topography; components are often lobate, suggesting the presence of lava flows; boundaries between bright and dark material are sharp; domes and radar-dark features are present locally. Transitional with bright plains.
Digitate plains	Composed of alternating elongate lobes of radar-bright and radar-dark material; both bright and dark material form a series of elongate flow-like features that extend for distances of 100's of km; boundaries between dark and bright material are sharp.
Stippled plains	Characterized by a "salt and pepper" appearance at a scale of a few km; stippling is relatively uniform over 100's of km; slight degree of mottling on the scale of 1000's of km; transitional variations between bright and dark material. Found in the lowlands of Helen Planitia.
Linear deformation zones	Groups of closely spaced radar-bright lineaments of several types arrayed in linear zones: (1) Ridge belt-like zones – spacing of lineaments of 10 to 40 km with belt width of 75 to 250 km; lineaments are parallel to interbraiding; several belts occur on locally elevated topography; similar to ridge belts in the northern hemisphere; occur predominantly in Lavinia Planitia; interpreted to be compressional in origin. (2) Lineament patches – equidimensional regions of short 20 to 40 km long radar-bright lineaments; patches are typically polygonal with dimensions of 1500 km or less; individual lineaments are spaced from 15 to 20 km and are separated by regions of plains. (3) Parallel paired lineaments – characterized by two wide (15 to 40 km) radar-bright bands separated by a region of radar-dark material; width of the lineament zone ranges from 60 to 100 km with lengths of 250 to 450 km commonly occur radial to some edifices (Innini and Hathor Montes); interpreted as graben.
Tessera	Characterized by a complex system of intersecting radar-bright and dark lineaments; corresponds to regions of locally elevated topography (0.5 to 2.0 km above the surrounding plains); lineament spacing of 5 to 10 km with lengths of 20 to 100 km; small patches of dark plains located within the unit; boundaries with adjacent plains are distinct. Complex structural origin perhaps involving a variety of tectonic processes (Bindschadler and Head, 1990).

TABLE I. (Continued).

Unit	Characteristics
Edifices	Large sub-circular features with positive relief; diameters of 100 to 300 km; surrounded by radar-bright and dark lobate deposits that extend outward for up to several hundred km; outer boundary often digitate; in some edifices a circular to oval region of radar-dark material is located at the summit (Ushas Mons); interpreted as volcanoes.
Circular features	
Ovoids	Quasi-circular to oval features with diameters greater than 100 km; characterized by one or commonly two narrow radar-bright rings; bounding ring is often elevated and ring width ranges from 15 to 20 km; interior of the features contains plains and occasionally domes; ovoids are frequently associated with lineament zones; large features appear to be coronae; interpreted primarily as locations of mantle upwelling; "hot spots".
Ovoid chains	Groupings of ovoids forming a "beaded" chain of a series of closely packed structures; located in Themis Regio; in several locations an edifice is present within the ring structure. Some of the ovoids are irregular in shape and some are cut by radar-bright lineaments and possibly separated. Interpreted as location of mantle upwelling associated with zones of extension.
Structures	
Craters	Circular features with distinct radar-bright rims; some have central peaks while others have interior rings, typically surrounded by a radar-bright annulus extending from 1 to 4 crater radii from the rim; exterior deposits are sometimes asymmetrical; locally some craters are found within dark-halo deposits. Interpretation to be craters of impact origin.

in Guinevere Planitia (Senske *et al.*, 1991). Since this unit is located in a region imaged at low incidence angles (Figure 2a), the distinctiveness of the unit may be due in part to the topographic features preferentially seen at these incidence angles. However, on the basis of PV data (Head *et al.*, 1985) this region also appears to be a transition from rough plains of intermediate reflectivity to the north, to smooth plains of intermediate reflectivity to the south. *Digitate plains* are composed of bands and patches of alternating radar-bright and radar-dark material, interpreted to be lava flows. This unit is found exclusively along the northern edge of Lada Terra and its extension to Alpha Regio and is typically associated with lineament belts. Lava flows making up this unit originate in the vicinity of linear deformation zones and extend for distances of hundreds of km into the lowlands of Lavinia Planitia. On the basis of PV data (Head *et al.*, 1985) these plains appear to have anomalously low reflectivity and low to intermediate roughness, perhaps due to an abundance of diffuse scatterers (Bindschadler and Head, 1988). Areas showing characteristics similar to the digitate plains are seen south of Lakshmi Planum in the northern high latitudes (Stofan *et al.*, 1987). The lowlands of Helen Planitia are characterized by an extensive unit of *stippled plains* having a 'salt and pepper'-like radar backscatter pattern with few tectonic features present. The stippled plains are relatively uniform throughout Helen Planitia. On

the basis of PV data (Head *et al.*, 1985) these plains appear to be relatively smooth at radar wavelengths and to have intermediate to high reflectivity values.

On the basis of their characteristics (presence of flow-like subunits, embayment relationships, presence in lows, etc.) and associated features (domes, flows associated with vent-like features and fissures, etc.) the plains units are interpreted to be volcanic in origin. Although viewing geometry and signal-to-noise factors must be considered, the distinctiveness of the distribution of the bright, dark and stippled plains suggests that their surfaces have different roughnesses and textures that may be linked to eruption conditions and environments (Head and Wilson, 1986; Greeley and Martel, 1988) or subsequent degradation (Farr and Anderson, 1987; Kryuchkov and Basilevsky, 1989). The radar-bright parts of the digitate plains show the most distinctive flow-like features and appear to be the youngest flow unit on the basis of sharpness of definition and local superposition. A bright plains unit is concentrated in the area of eastern Lavinia where the digitate plains occur and this may be evidence that the unit is relatively young compared to the dark plains elsewhere in the mapped area. Examples of individual radar dark flows superposed on radar bright units in this region and elsewhere (Stofan *et al.* 1987; Roberts and Head, 1990) indicate that there are exceptions to the general radar darkening with time trend (Kryuchkov and Basilevsky, 1989).

Groups of closely spaced generally parallel radar-bright lineaments forming belts define **linear deformation zones** which are located in four distinct regions: (1) Phoebe Regio and the northwest flank of Hathor Mons, located along a N 45° W trend, (2) along an approximate north-south trend extending south from Hathor Mons, (3) in Lavinia Planitia in two trends (WNW–ESE, NE–SW) together forming a fan pattern whose apex is centered near 45° S and points east and (4) the linear belt at the northern edge of Lada Terra oriented ENE–WSW. A fifth major belt, located in Themis and trending WNW–ESE, is mapped here as an ovoid chain, but contains numerous linear features. Linear zones of deformation also occur along the NW margin of Alpha Regio and between Lada and Alpha Regio. The detailed characteristics of the lineament belt components is portrayed in the tectonic map (Figure 2e). Lineaments are interpreted to be due to enhanced surface roughness associated with individual faults or folds and are thus viewed as tectonic in origin. Although broadly similar at the scale of this map (Figure 2d) the lineament belts differ in their detailed characteristics and probably in the sense of strain indicated by their linear features. For example, the morphology of many of the lineament belts is similar to ridge belts mapped in the northern high latitudes often interpreted to be compressional in origin (Kryuchkov, 1989; Frank and Head, 1990a; Frank and Head, 1990b), while others appear similar to extensional faults associated with rift zones such as at Devana Chasma in Beta Regio (Campbell *et al.*, 1989). The belt of lineaments located along the western edge of Alpha Regio is similar to the association of ridge belts and tessera observed at Tellus Regio. The origin of individual occurrences of lineament belts is discussed in subsequent sections.

On the basis of their topography and the presence of radar-bright flows, **edifices** are interpreted to be volcanic constructs. They are found associated with linear deformation zones in Phoebe Regio, Themis Regio, the region made up of Ushas, Innini and Hathor Montes and along a linear trend extending to the southeast toward Lada Terra from Eve. The edifices possess a variety of characteristics; Ushas Mons shows a structure similar to the volcano Sif Mons (Campbell *et al.*, 1989; Senske, 1990), while edifices mapped in the vicinity of Tefnut Mons show evidence of large caldera structures and are more similar to Colette and Sacajawea (Pronin *et al.*, 1986; Roberts and Head, 1990).

Two occurrences of **tesserae** are mapped: (1) Alpha Regio and (2) a feature located along the northern edge of Lada Terra (Figures 2b, d). Alpha possesses characteristics of tessera mapped elsewhere in the northern high latitudes of Venus. The presence of Alpha as the only significant region of tessera in this part of the planet, a much lower percentage of tessera occurrences than in the northern high latitudes (Bindschadler and Head, 1989; Sukhanov *et al.*, 1989), suggests that mechanisms that form tessera may not be as dominant in this part of the planet, or that additional occurrences of tessera terrain underlie the plains. Embayment relationships of plains and tessera and abrupt truncation of tessera trends at the plains boundary suggest that the tessera may underlie additional portions of the region.

A number of features identified as **ovoids** or corona-like features are mapped in the southern hemisphere. Ovoids have two modes of occurrence: (1) small ovoids occur in the low lying plains and (2) larger ovoids occur along linear deformation zones and form ovoid chains. The grouping of ovoids in Themis Regio and the chain of structures extending southeast from Eve are broadly similar to clusters of circular features seen elsewhere on the planet (Beta-Eistla deformation zone, Mnemosyne Regio) (Stofan *et al.*, 1990a; Stofan and Head, 1990). The region mapped as an **ovoid chain** corresponds to Themis Regio and is characterized by a system of interconnecting circular to oval features, which in some places are cross-cut by lineament belts (Stofan *et al.*, 1985; Stofan *et al.*, 1990b). In some places when the lineaments are removed, the oval can be restored to a more circular shape, suggesting that the features have undergone extension (Campbell *et al.*, 1991). The presence of features associated with the ovoid chain and interpreted to be volcanic edifices suggests that volcanism along with tectonism plays a role in the formation of this unit. Other larger ovoids or coronae-like features occur along the lineament belt bounding northern Lada Terra and extending from there to Alpha Regio. In particular, an 800 to 1000 km corona feature occurs to the south of this chain in Lada Terra (Campbell *et al.*, 1991). Ovoids and coronae (Stofan and Head, 1990; Pronin and Stofan, 1990) have several characteristics in common and are discussed in more detail in subsequent sections.

Craters of apparent impact origin have been mapped in this area (Figure 2c) (Table II) and the largest one (Lise Meitner) is shown on Figure 2d. The craters

TABLE II

Craters of the Venus southern hemisphere

Latitude	Longitude	Diameter (km)	Morphology
−10.79°	11.76°	39	CP, DE-A(S)
−11.46°	342.41°	18	S
−12.05°	5.04°	12	S
−16.74°	347.48°	19	CP, BE
−17.82°	349.10°	21	DF, DE-A(SE)
−20.46°	357.21°	13	S
−21.90°	317.16°	42	CP, BE-A(NW)
−22.05°	342.78°	18	DF
−22.68°	306.47°	29	CP, DE-A(SW)
−22.70°	324.18°	32	DF
−23.07°	300.05°	27	DF, DE-A(SW)
−24.12°	295.74°	33	CP
−24.19°	344.18°	41	CP, BE-A(SW)
−24.74°	296.11°	48	CP, DE-A(W)
−25.55°	317.49°	30	DF, DE
−26.40°	337.28°	50	OCP(NW), DF, BE-A(SE)
−26.50°	356.56°	32	CP, DF
−26.51°	339.97°	66	OCP(SE), DF, BE-A(N)
−28.59°	18.83°	18	CP, DE
−28.62°	337.18°	40	CP, BE-A(SE)
−28.97°	294.30°	30	CP, DF
−29.33°	310.61°	22	CP, DE-A(W)
−32.20°	314.96°	33	CP, DF, DE-A(S)
−38.27°	331.52°	11	S
−38.58°	274.80°	37	CP, DE-A(NE)
−42.08°	271.95°	42	CP, DF, DE-A(NW)
−44.43°	271.09°	53	CP, DF
−44.85°	337.76°	22	CP, BE
−45.27°	348.95°	11	S
−45.57°	335.53°	44	CPR, DF, BE
−46.20°	314.81°	41	CP, BE-A(NW-SE)
−46.66°	285.68°	13	CP
−46.72°	12.90°	28	CP
−47.65°	325.73°	8	S
−47.85°	277.75°	25	CP, DE
−52.43°	329.51°	59	CPR, DF, BE-A(SE)
−54.97°	312.85°	12	S
−55.66°	321.75°	157	MR,DF,DE-A(NE)
−56.05°	298.48°	12	S, DE
−57.69°	298.79°	8	S
−59.53°	354.47°	71	DF, DE-A(S)
−60.50°	304.89°	12	S
−63.10°	289.32°	43	CPR, DF, BE-A(S)
−51.99°	36.72°	36	CP, BE-A(S)
−54.34°	18.96°	48	DE, BE-A(SW)
−54.87°	305.51°	15	S, DE
−56.29°	295.47°	12	S
−57.96°	13.27°	30	CP, DE
−66.60°	270.56°	15	S
−68.21°	315.51°	13	S
−69.98°	319.98°	17	S
−78.07°	309.47°	35	CP, DF, BE-A(W)

Crater Morphologic Classification.

S – Simple Crater

Crater Interior:

CP – Central Peak
OCP – Offset Central Peak (with offset direction)
CPR – Central Peak Ring
MR – Multi-ring
DF – Dark Floor

Crater Exterior

BE – Bright Ejecta
DE – Diffuse Ejecta
BE-A – Asymmetric Bright Ejecta (with offset direction)
DE-A – Asymmetric Diffuse Ejecta (with offset direction)

are distributed relatively evenly across the surface (Campbell *et al.*, 1990; Campbell *et al.*, 1991) despite some clustering, typically in the lowlands (southern Guinevere Planitia, southern Navka Planitia), with the upland containing Ushas, Innini and Hathor Montes, Themis Regio and Alpha Regio showing slightly lower concentrations. In comparison, there is a slightly higher concentration of craters on highlands (Beta Regio, Western Eistla Regio) in the equatorial region. This observation suggests that highlands in the southern hemisphere are relatively young, while those in the equatorial region preferentially retain craters and possibly preserve some older surfaces. There are no obvious regions of significantly higher or lower crater density in the southern hemisphere, indicating that the use of craters to determine age and stratigraphic relations between the different units may not be appropriate here.

On the basis of superposition and cross-cutting relationships local relative ages can be ascertained, but regional unit stratigraphy is not clear and thus it is premature to construct a stratigraphic column for the mapped units in this region. Locally, plains clearly embay the tessera of Alpha Regio and volcanic edifices and flow units are superposed on lineament zones in Ushas, Innini and Hathor Montes. The fractures of the lineament belts are interpreted to be relatively young due to their enhanced surface roughness and often cross-cutting of the plains and it is clear that the digitate plains often originate from lineament zones, covering them in part, and are superposed on plains in Lavinia, as well as flowing around lineament zones there. Thus, processes of volcanism and tectonism appear to have operated concurrently during the formation and evolution of this region.

2.3. Tectonic elements and their distribution

Individual tectonic elements (lineaments) of three types have been mapped (Figure 2e): (1) radar-dark lineaments (dashed pattern), (2) radar-bright and diffuse (dotted pattern) and (3) radar-bright and distinct (solid line). The most abundant tectonic features in the southern hemisphere are radar-bright lineaments. These features are typically grouped into lineament belts and can be parallel to interbraided within the belts (compare Figure 2b, d, e). Most of the lineament belts occur in a region where the incidence angle is greater than 25°, and it is thus difficult to determine uniquely if they are ridges, troughs, or scarps. On the basis of high resolution data in other areas and knowledge of terrestrial environments, the linear features are likely to consist of: (1) linear fault scarps or collections of scarps with surface roughness enhanced by rubble; these often occur in extensional and rift environments and may be simple graben and/or represent the surface manifestation of subsurface dike intrusion (Wilson and Head, 1988); (2) ridges or fault scarps formed in compressional environments (anticlines, thrusts) and enhanced by surface roughness; and (3) strike-slip faults. The similarity of some of the lineament belts to ridge belts (particularly Antiope, Hippolyta and Molpadia Lineae in Lavinia Planitia) suggests that many of these features may be ridges. In areas where bright lineaments form parallel, often paired patterns, for example

on the flanks of Hathor Mons, the structures show characteristics similar to features interpreted elsewhere as fault scarps of extensional origin (Beta Regio; Stofan *et al.*, 1989). Located along the northern edge of Lada Terra are systems of radar-bright lineaments that are parallel and extend for distances of 100's to 1000's of Km and separated by distances of 10 to 20 km. One such set of lineaments forms a pattern possibly radial to the 1000 km diameter corona feature in central Lada Terra (Campbell *et al.*, 1991). This association and pattern suggests that some of the lineaments are fractures or faults. The end segments of a number of the radar-bright lineaments are mapped as bright diffuse structures. In regions where bright diffuse lineaments are associated with both lineament belts and features interpreted to be fractures, it appears that the lineaments are partially covered by plains material. Within the southern hemisphere features mapped as dark lineaments are found mainly in Helen Planitia. Several dark lineaments are found to cut across the region of ovoids extending to the southeast from Eve. These structures are most likely faults or depressions that have been flooded by plains material. Later we examine detailed examples of lineament belts to assess possible modes of origin in these areas and we assess the spacing of lineaments from local environments as an aid in the interpretation of their origin.

Assessment of the tectonic map (Figure 2e) shows many instances where there is a strong correlation of linear trends with directions normal to local illumination azimuth (compare Figures 2a and 2e). For this reason, we have not compiled a lineament azimuth-frequency (rose) diagram, but instead discuss the broad trends of linear structures that clearly are not dominated by viewing geometry. This analysis reveals several patterns, including: (1) the distinct concentration of structural elements in the tessera of Alpha Regio (the areal deformation of Basilevsky *et al.*, 1986), (2) the termination of the linear deformation zones extending south from the rifts of Phoebe Regio, (3) the NNE–SSW trend extending from Ushas Mons south, (4) the central WNW–ESE broad trend from Themis, through the belts of Lavinia, terminating against (5) the NNE–SSW trending belt along the eastern border of the map area, (6) the ENE–WSW trend along the northern edge of Lada Terra and (7) the chevron-shaped trend apparently superposed on the belt at the northern edge of Lada and possibly related to the large corona to the south (Campbell *et al.*, 1991). Although regional trends crosscut each other in several instances, in most cases it has not yet been possible to establish relative ages or to establish whether one trend consistently predates or postdates another. Exceptions are the chevron structure (7) which appears to be superposed on the trend at the northern edge of Lada (6) and which in turn is partly obscured by units of the digitate plains and elements of the trend at the eastern edge of the mapped area (5) where extremely long bright lineaments along its western edge cut the dark plains and both cut and are overlain by the digitate plains. Thus, candidates for some of the youngest tectonic activity are located in the southeastern part of the mapped area.

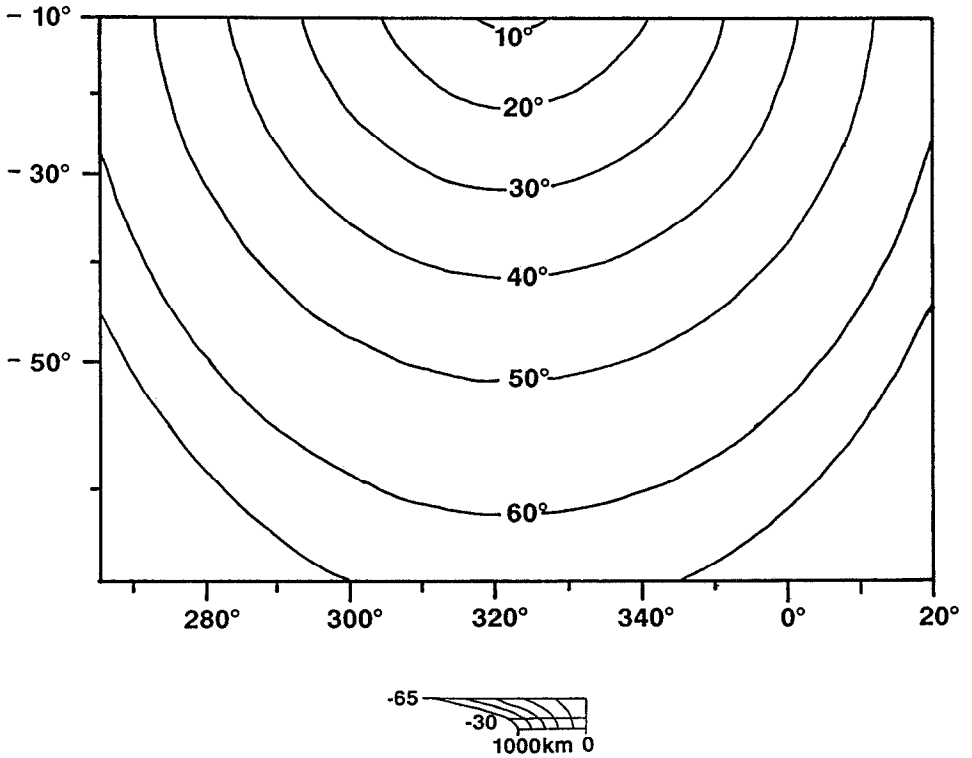

Fig. 2(a). Map showing lines of constant incidence angle for the southern hemisphere image data. The look direction is perpendicular to these arcs. For the range of angles shown here, the radar is primarily sensitive to topographic slopes (quasi-specular scattering) at low southern latitudes and wavelength-scale roughness (diffuse scattering) at high southern latitudes.

3. Regional Analyses

In this section we assess a number of regions (Figure 2c) in more detail in order to examine their geologic and tectonic characteristics and their relationships. These regional analyses permit a further understanding of the geologic processes responsible for the formation of the mapped units and structures (Figure 2).

3.1. Phoebe regio

The southern part of Phoebe Regio (Figures 1 and 3) extends from the northwest corner of the imaged area and is characterized as two elongate topographic rises striking northwest to southeast for 1000 to 1500 km, with superposed radar-bright lineament zones 200 to 400 km wide (Figure 2b). The northward extension of these lineaments and the rises correspond to the location of deep troughs first identified as possible rifts in Goldstone images (Goldstein *et al.*, 1976; McGill *et al.*, 1981). In Pioneer Venus altimetry maps and SAR images the two rises of

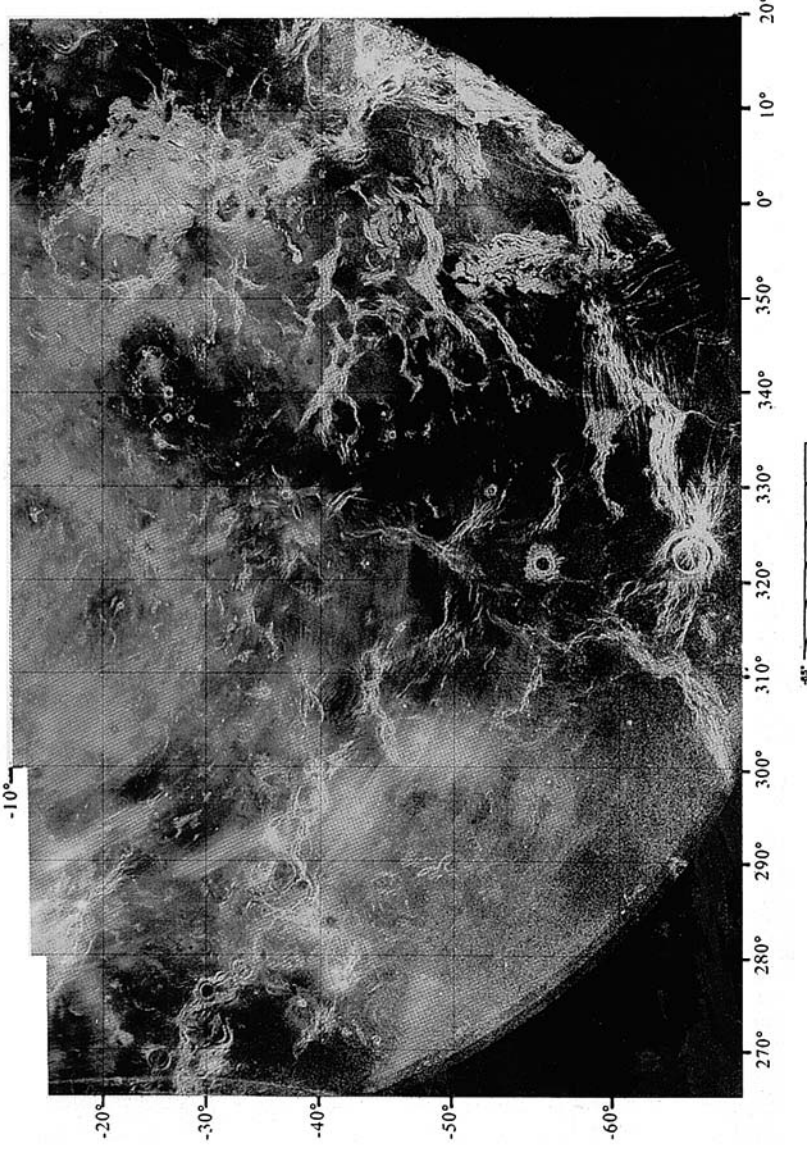

Fig. 2(b). Arecibo radar image of the Venus southern hemisphere. The bright whispy feature centered near 45° S, 295° is an artifact.

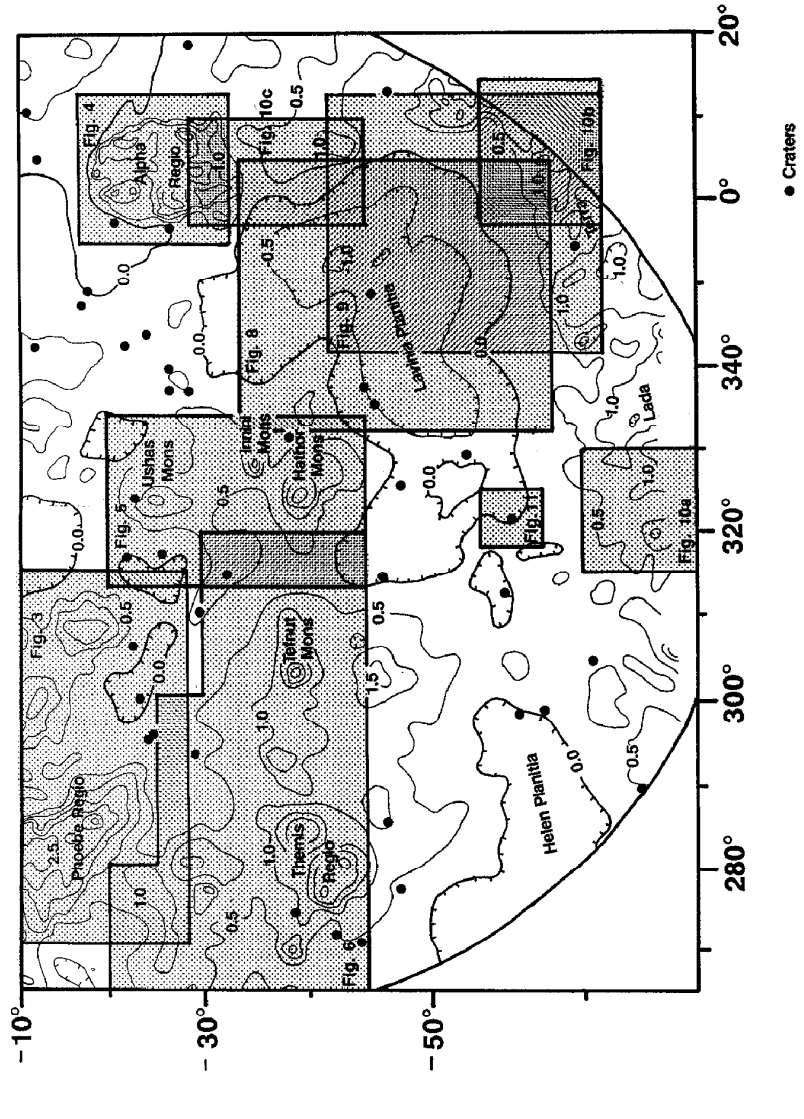

Fig. 2(c). Map of Pioneer Venus topography, contoured at 500 m intervals, of the portion of the southern hemisphere imaged by Arecibo. The shaded areas correspond to regions discussed in the text. The black dots indicate the location of impact craters.

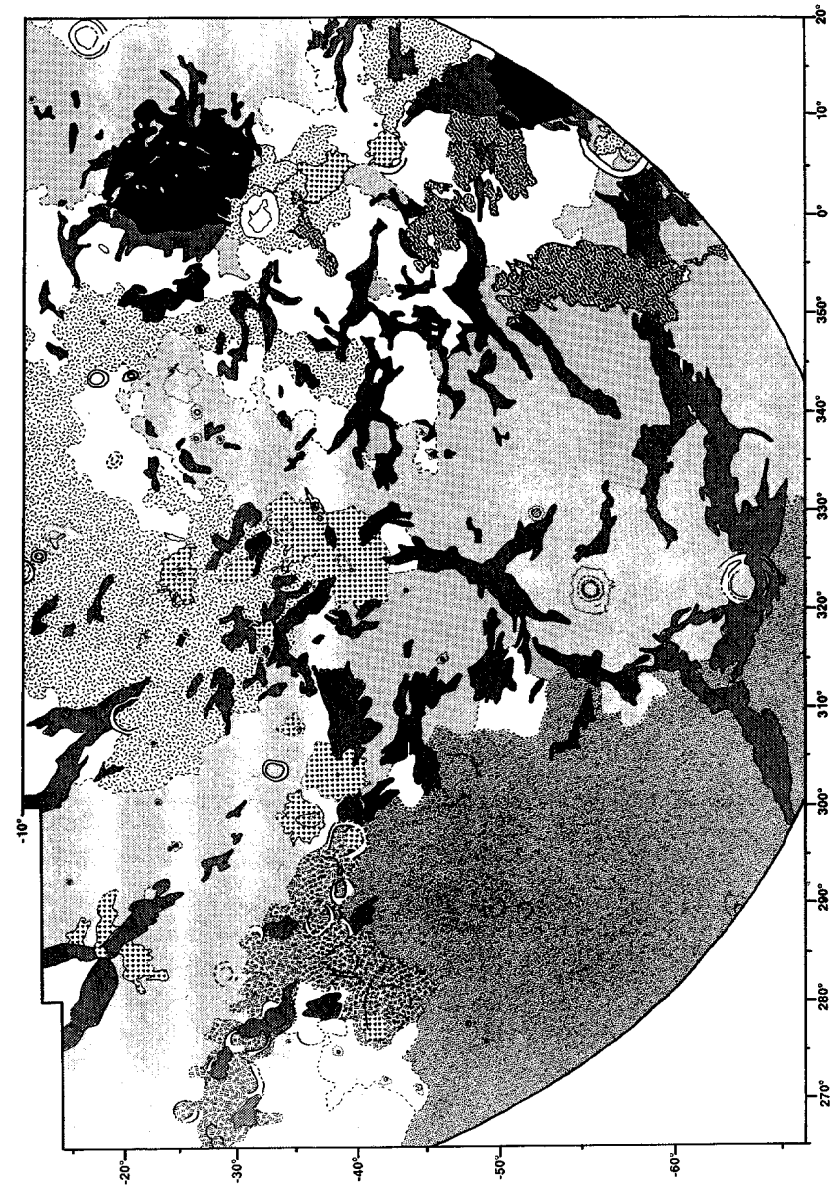

Fig. 2(d). Geologic map of the Venus southern hemisphere. Like the northern high latitudes and equatorial region, the most abundant unit in this part of the planet is plains. Unit descriptions are given in Table I and their characteristics are discussed in the text.

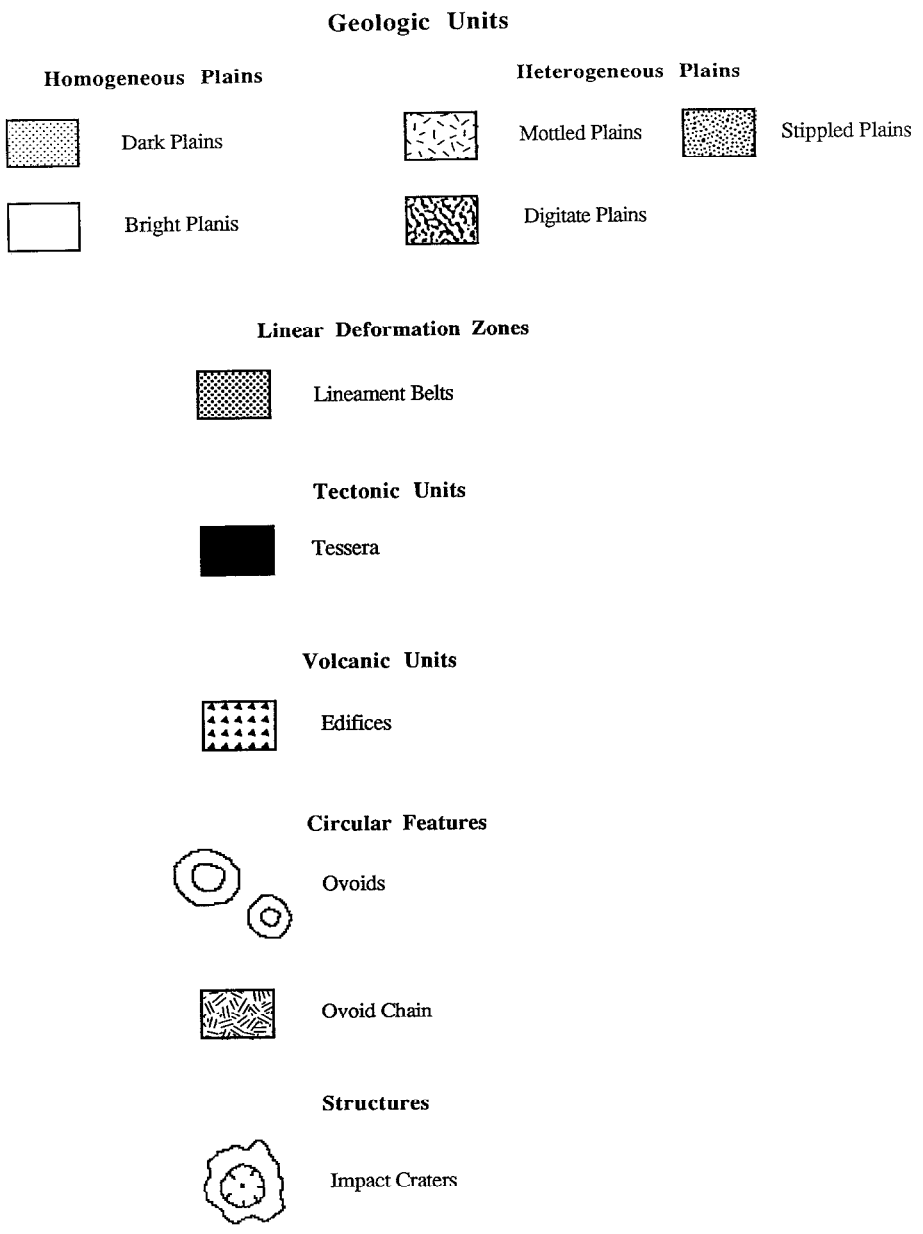

Fig. 2d (Continued).

Phoebe Regio are shown to merge at the equator into a single feature which connects northward via a transfer zone with similar radar bright lineaments at the southern end of Beta Regio at Devana Chasma (Figure 3). Devana Chasma is a deep trough extending through Beta Regio and has been interpreted to be a rift resulting from regional doming and extension (McGill *et al.*, 1981; McGill *et al.*,

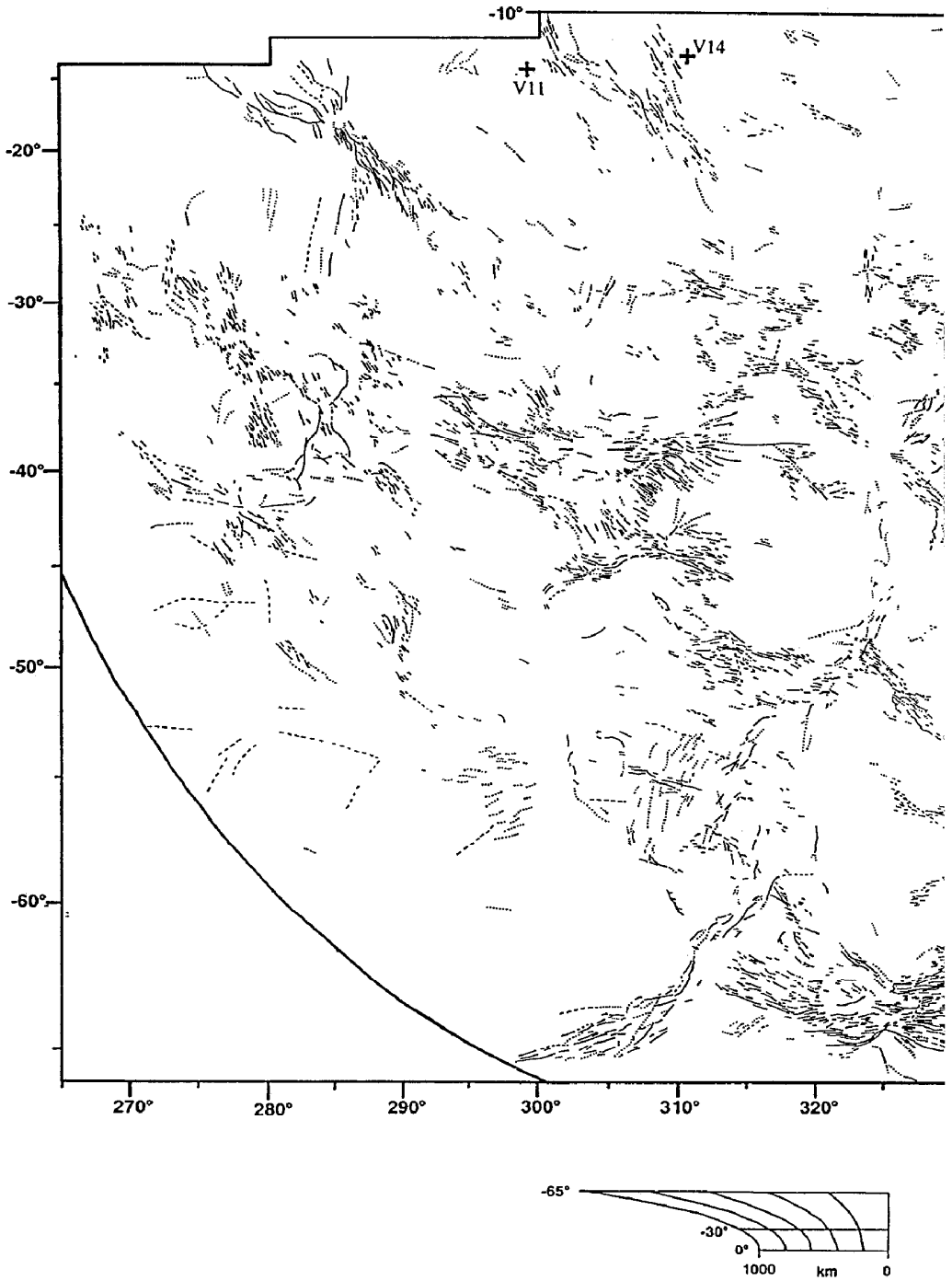

Fig. 2(e). Lineament map of the Venus southern hemisphere. The principle zones of lineaments are concentrated in Lada Terra, Lavinia Planitia, Themis Regio, Phoebe Regio and the upland of Ushas, Innini and Hathor Montes (see Figure 2c for region locations). The location of Venera landers 8, 11 and 14 are labelled "V8", "V11" and "V14".

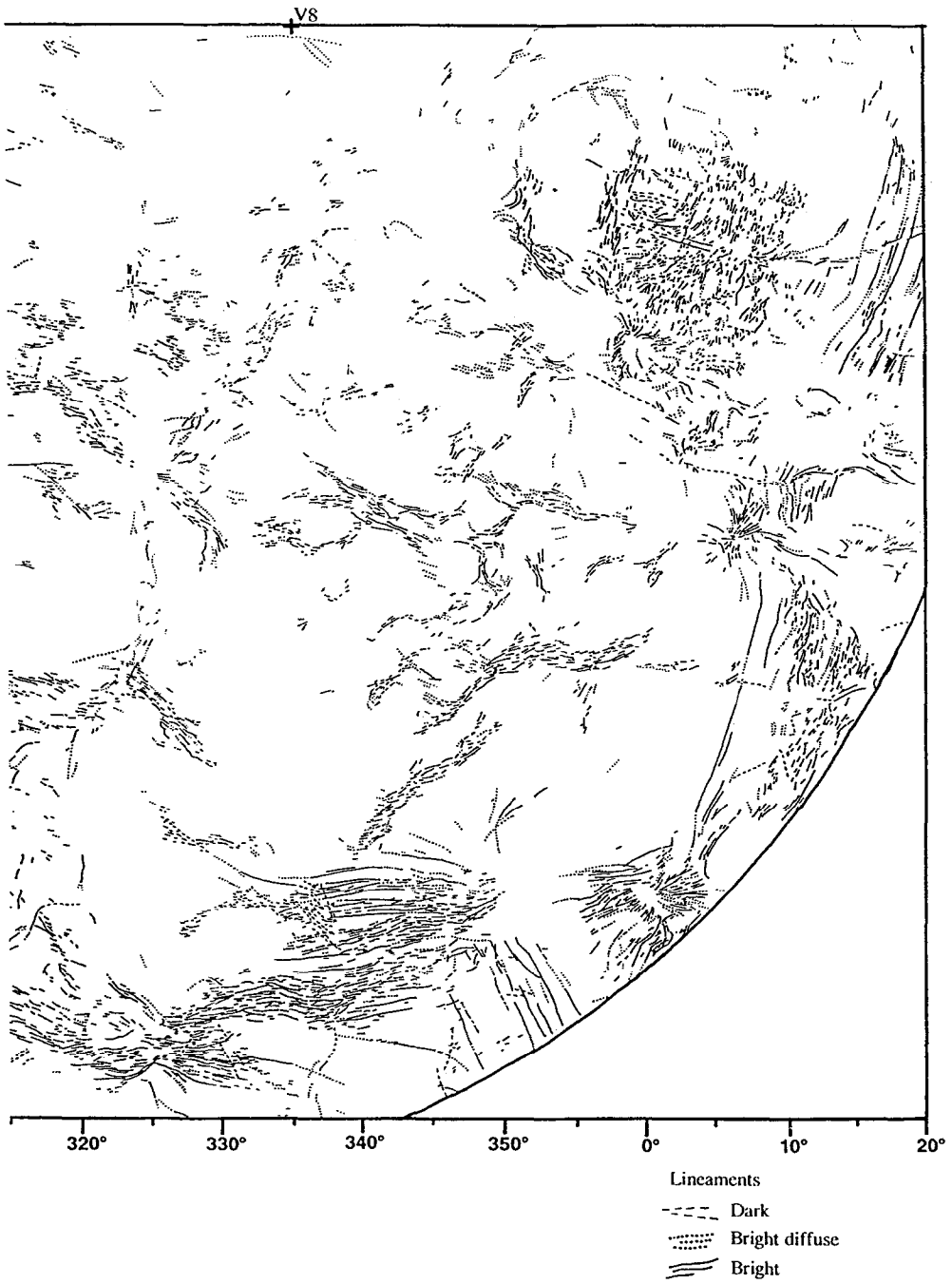

Fig. 2e (Continued).

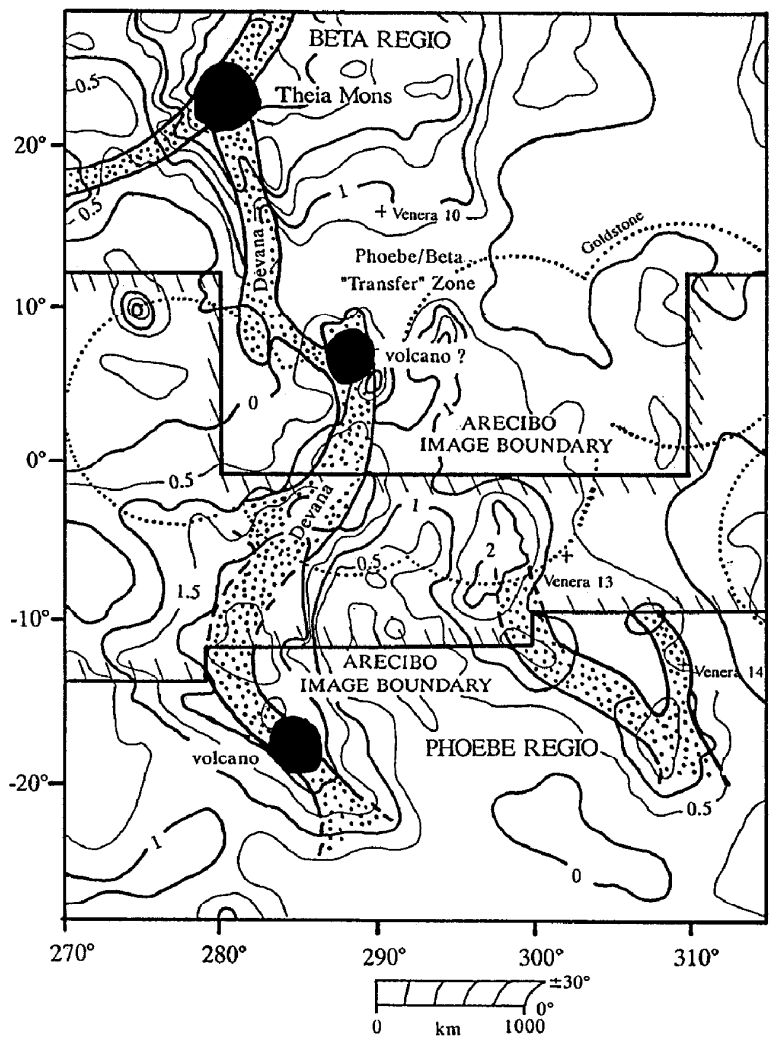

Fig. 3. Sketch map of Phoebe Regio showing the continuation of Devana Chasma from the equatorial region into the southern hemisphere where it is mapped as a linear deformation zone (see Figure 2d). The topography is from Pioneer Venus and is contoured at 500 m intervals. Edifices are located at the points where Devana terminates or links up with other lineament zones. The dotted circles indicate the location of Goldstone radar image data used to extend the trend of Devana Chasma into the southern hemisphere.

1983; Campbell *et al.*, 1984; Campbell *et al.*, 1989; Stofan, *et al.*, 1989). This interpretation is consistent with analyses of gravity anomalies over Beta and Phoebe Regiones (Esposito *et al.*, 1982; Reasenberg *et al.*, 1981) and the presence of numerous closely-spaced radar bright lineaments interpreted to be fault scarps and bright radial centers interpreted as large volcanoes (Figure 2d). A variety of observations therefore suggest that Beta Regio and Phoebe Regio are linked and

that both regions are characterized by extension, rifting, large positive gravity anomalies and volcanism.

The western arm of the two lineament systems in Phoebe Regio is brighter (and observed at somewhat higher incidence angles) than the eastern arm, but the total number of lineaments, their individual length and their curvature are similar in both arms. The lineaments of the western arm appear continuous for up to 400 km, but merge into a single radar bright feature at about 17° S (Figures 2d and 3) similar in radar characteristics to the volcano Theia Mons in Beta Regio (Campbell *et al.*, 1989). Southeastward of this volcano the lineaments again fan out, become more numerous and assume anastomosing patterns. The lineaments ultimately diminish and splay southward into the lower plains in a manner analogous to the northern terminus of Devana Chasma in Beta Regio (Stofan *et al.*, 1989).

The eastern arm is somewhat more subdued in overall backscatter cross section and consists of short anastomosing bright lineaments. At about 17° S the lineament zone bifurcates with another short arm extending north for several hundred kilometers. South of 17° S the lineaments merge to form a single zone 300 km wide and 400 km long which gradually merges with the lower plains. At the point where the lineaments merge with the plains, 200 degrees of arc of a single large ovoid are superposed on and appear to terminate the lineament zone. Numerous bright small domes occur in the transition between the lineaments and the elevated topography and the low plains. Several parallel linear streaks striking east-northeast occur along the eastern margin of the eastern lineament arm (between 15° S/310° to 20° S/312°) and may be the traces of lava flows flowing down regional east-northeast gradients away from the Phoebe rifts.

The along-strike projection of the two arms of the Phoebe Regio lineament/rift system intercepts several lineaments in the low plains lying generally between and to the west of Ushas and Hathor Mons. However, lineaments in the southern tip of the western arm where it splays into the plains generally trend north-south in orientation and a physical basis for the alignment of the Phoebe lineaments and the Ushas/Hathor lineaments is uncertain.

3.2. Alpha Regio

Alpha Regio (17° S to 33° S; 355° to 13°), a 1300 × 1500 km rectangular upland region averaging about 1 km (and rising up to 3 km) above the surrounding plains, is the most prominent feature in the mapped portion of the southern hemisphere of Venus by virtue of its high roughness and reflectivity (Campbell and Burns, 1980) (Figures 2c, 4a–c). On the basis of its properties in PV data (Bindschadler *et al.*, 1990) and low resolution images, it was predicted to be tessera and these images confirm this interpretation. The area south of Alpha Regio, which includes the ovoidal feature Eve, is marked by a relatively complicated lineated terrain some of which appears to be a continuation of the tessera pattern in Alpha. Alpha is divided into northern and southern sections by a prominent N 65° W topographic trend and radar-bright lineament. The total area of tessera terrain is approximately

1.4×10^6 km^2 (about one-tenth of the area of the northern hemisphere tessera occurrence).

Alpha Regio is characterized by a series of alternating radar bright and dark linear features that are oriented in several major directions (Figure 4d, e). These features are similar to the tessera fabric seen in Venera 15–16 data where the alternating bands mark the location of parallel ridges and troughs (Basilevsky *et al.*, 1986). In Alpha, the most abundant and prominent orientation is N 20° E approximately parallel and orthogonal to the edges of Alpha. Linear elements with this trend in the northern half of Alpha are spaced between 18 and 28 km apart (average of 20 km) and have lengths ranging from 10 to 75 km (averaging 33 km). Those in the southern part are spaced 15 and 20 km apart (averaging 17 km) and range in length from 10 to 150 km (averaging about 35 km). Western Alpha is characterized by a similar trend of parallel lineaments which have been mapped as a distinctive lineament zone (Figures 2d and 4b). Western Alpha is relatively lower (average elevation of 0.28 ± 0.60 km) and the spacing in western Alpha differs from that of Alpha proper, ranging from 12 to 18 km (averaging 14 km). Lineament lengths in the western Alpha lineament belt range from 15 to 110 km (averaging 50 km). A second major trend is oriented N 70° E and is particularly well developed in southern Alpha where it is part of a throughgoing system that connects with the lineament zone along the eastern edge of Alpha. Disruption of linear elements trending N 20° E occurs along this trend and it is common for these disrupted elements to be curved in toward the N 70° E trend in a manner suggesting right-lateral shear (Figure 4a–b, f). The third major trend is associated with the N 65° W trend that divides northern and southern Alpha. The zone is 50–100 km wide and is a topographic low dominated by two major bounding lineaments. It is floored by: (1) parallel short linear segments trending N 20° E and spaced relatively evenly and (2) a dark plains unit about 200 km long at its eastern edge. This zone is generally orthogonal to the N 20° E trend and separates northern Alpha (average elevation 0.79 ± 0.63 km) from southern Alpha (average elevation 1.34 ± 0.57 km).

Alpha Regio is surrounded by dark plains to the east and bright plains to the west (Figure 2d), both of which show embayment relationships with the tessera. High standing, oval-to-cigar-shaped intra-tessera plains are common within Alpha, with dimensions ranging from several tens of km and linear features about 100–200 km long and 50 km wide. The elongate patches of plains usually parallel the major structural trends and the smaller oval patches are often aligned along the structural trends (Figure 4a). These patches are similar to those mapped in Venera data at Laima Tessera and Tellus Regio (Basilevsky *et al.*, 1986; Sukhanov *et al.* 1989) and appear to postdate tessera formation.

Located just south of Alpha Regio is the 400–500 km oval structure Eve whose rim stands about 600–700 m above the surrounding plains. Eve is located at the northernmost end of a chain of ovoids and edifices (Figure 2d) and is separated from Alpha proper by plains, which also floor the interior of Eve. The bright rim

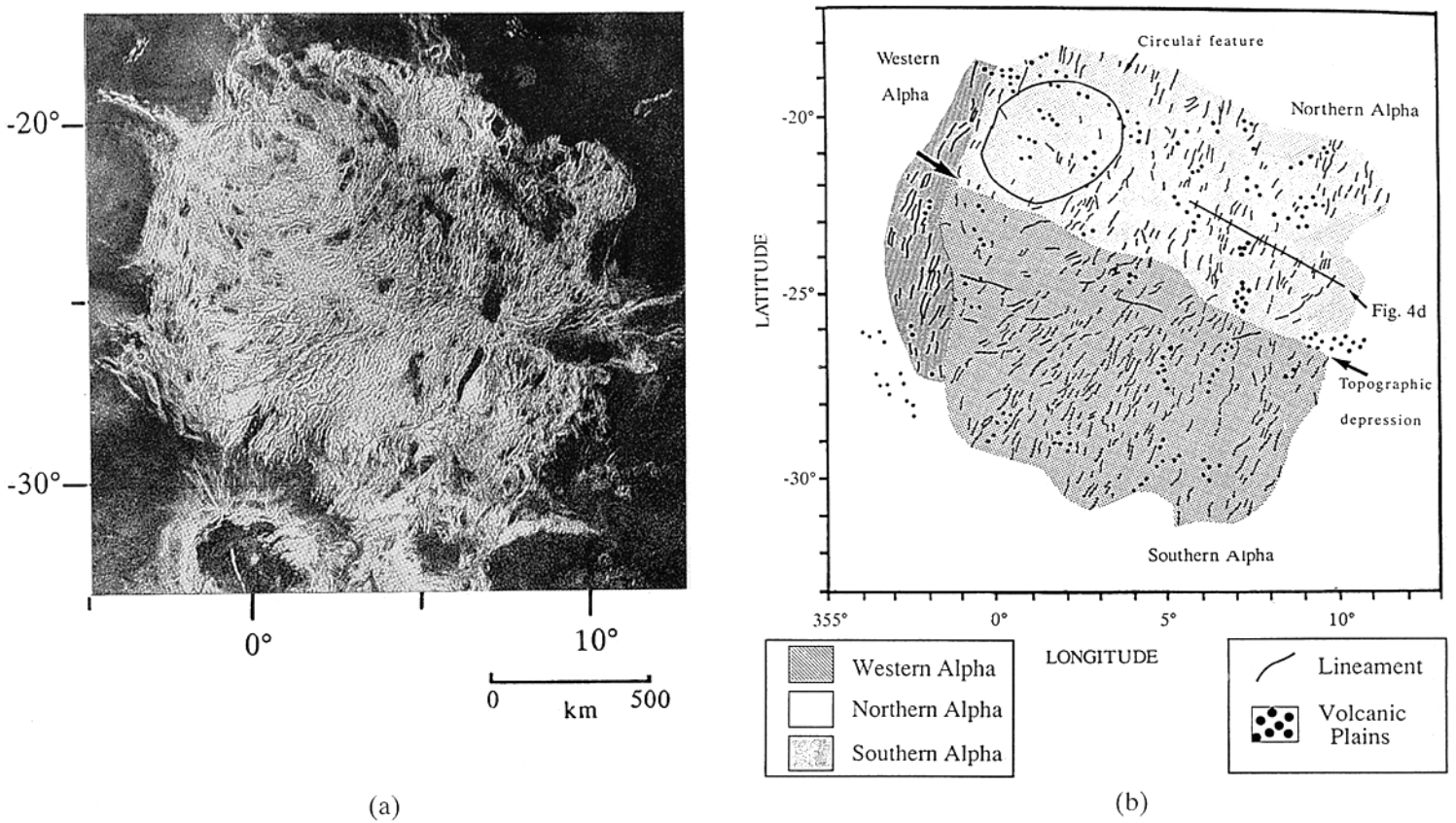

Fig. 4. Arecibo radar image (a) and sketch map of lineaments (b) in Alpha Regio. Lineaments, radar-bright/radar-dark pairs, are interpreted to be ridges and troughs. Lengths of lineaments are 10 km and greater with widths varying from 10 to 20 km. Intra-tessera plains of apparently volcanic origin are represented as large black dots. The tessera at Alpha Regio is divided into three units (western, northern and southern) based on Pioneer-Venus altimetry data and lineament azimuths. The location of the radar-brightness profile shown in Figure 4d is indicated in the upper right portion of Figure 4b.

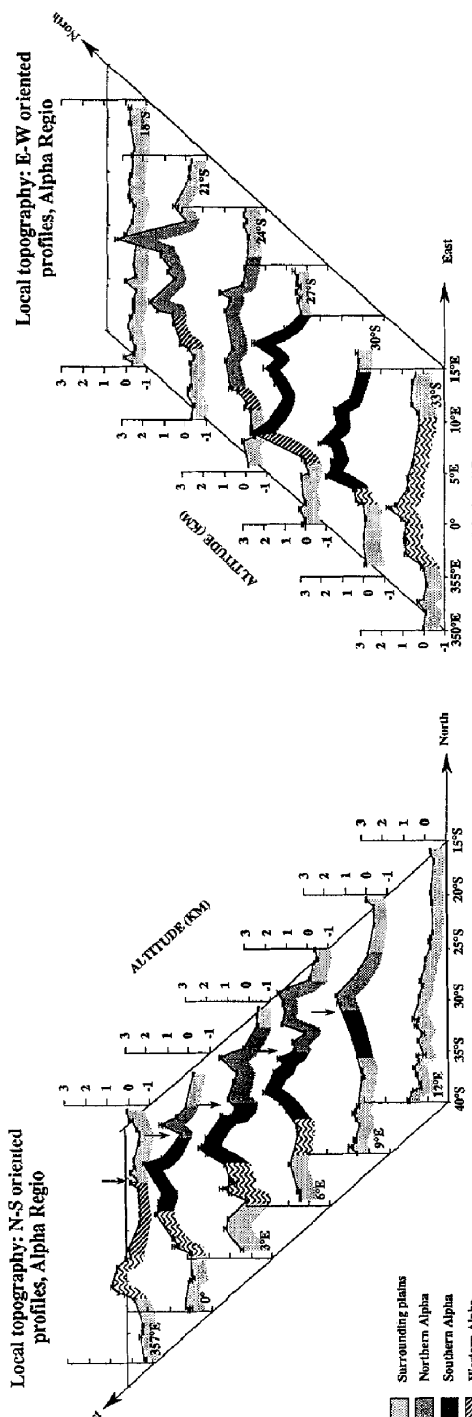

Fig. 4(c). North-south topographic profiles from 3° S to 12° S (spacing interval between profiles is 3° of longitude) are shown on the left part of the figure. Vertical arrows indicate the location of the topographic low that separates northern Alpha from southern Alpha. East-west topographic profiles from 18° S to 33° S (spacing interval between profiles is 3° of latitude) are shown on the left part of the figure. Individual Pioneer-Venus data points along with their error bars are shown. The profiles are shaded to match the units in Figure 4b.

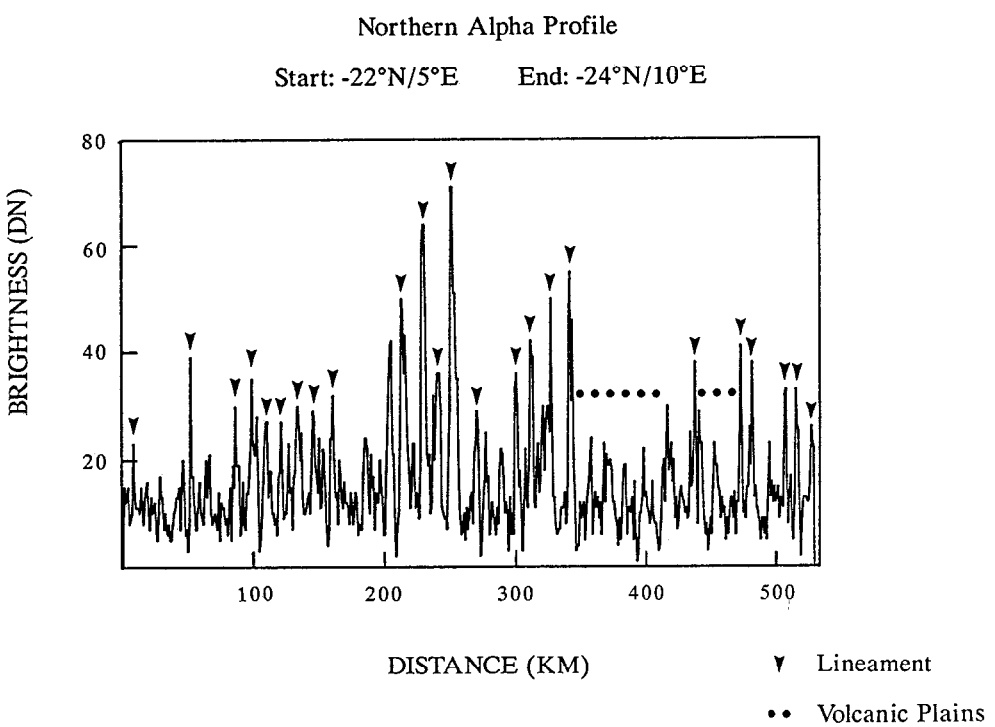

Fig. 4(d). Radar-brightness (DN) versus distance profile for NW trend within northern Alpha (see Figure 4b for location). Arrows indicate typical brightness levels and locations of radar bright/dark pairs that are used to calculate the spacing of lineaments.

of Eve is characterized by alternating ridges and troughs similar to those in Alpha. The orientation of many of these structures is similar to the N 20° E orientation common in Alpha, while others have other orientations. With the exception of a few N 20° W linear trends both inside and on the northern flank of Eve, virtually all of the structures are embayed by plains, as observed in Alpha proper. The presence of this tessera-like texture on the rim of Eve suggests that tessera may underlie larger regions of the area surrounding Alpha and may be covered by plains deposits. Although Eve has some of the characteristics of coronae (Stofan and Head, 1990; Pronin and Stofan, 1990), its origin has not yet been determined. Also unclear is the relation of Eve to the two oval structures just to the west of Alpha and to the 600 km diameter oval structure in the NW quadrant of Alpha associated with a local topographic high rising 1 km above its surroundings (Figure 4a–c).

Alpha Regio contains elements of both the "sub-parallel ridged" tessera subtype and the "trough and ridge" subtype of Bindschadler and Head (1991) and the "rhombic" and "orthogonal" subtypes of Sukhanov *et al.* (1989). There are a variety of models which may explain the fabric of the tessera, both involving extensional and compressional deformation (Bindschadler and Head, 1991). Al-

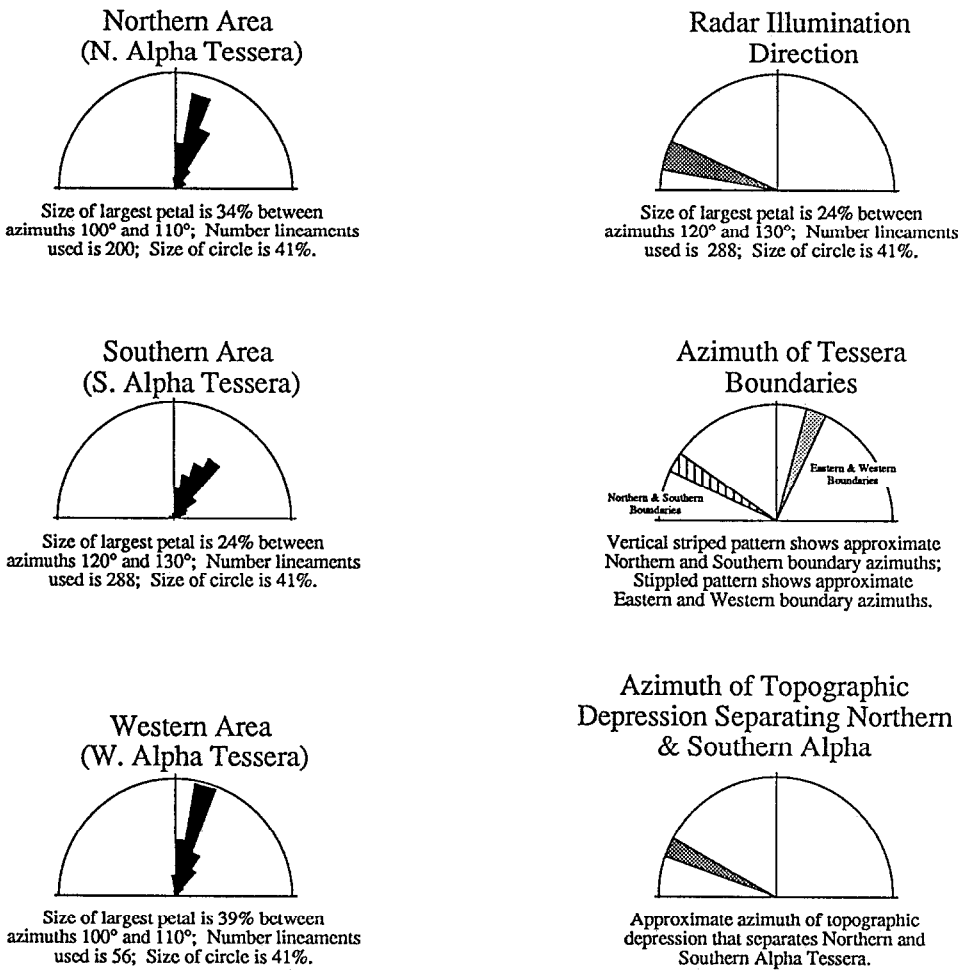

Fig. 4(e). Rose diagrams of lineament azimuths within Alpha (left part of the figure) and rose diagrams showing radar illumination direction, azimuths of tessera boundaries and azimuth of topographic low separating northern and southern Alpha (right part of the figure).

though the origin of high-standing tessera plateaus on Venus is not fully understood we outline two possible models for the formation of Alpha Regio. First, the model of Bindschadler and Head (1991) formulated to account for the sub-parallel ridged terrain involves compression to produce ridges and troughs, accompanied by strike-slip faulting. For Alpha, the direction of maximum compression would be perpendicular to the eastern and western boundaries of the tessera (i.e., WNW–ESE). This model is consistent with the following observations: (1) NNE–SSW strike of lineaments (interpreted to be anticlines and synclines); (2) the N 70° E trend of some lineations, interpreted to be strike-slip faults in accordance with this model, especially in the eastern half of Alpha; (3) formation of high-standing

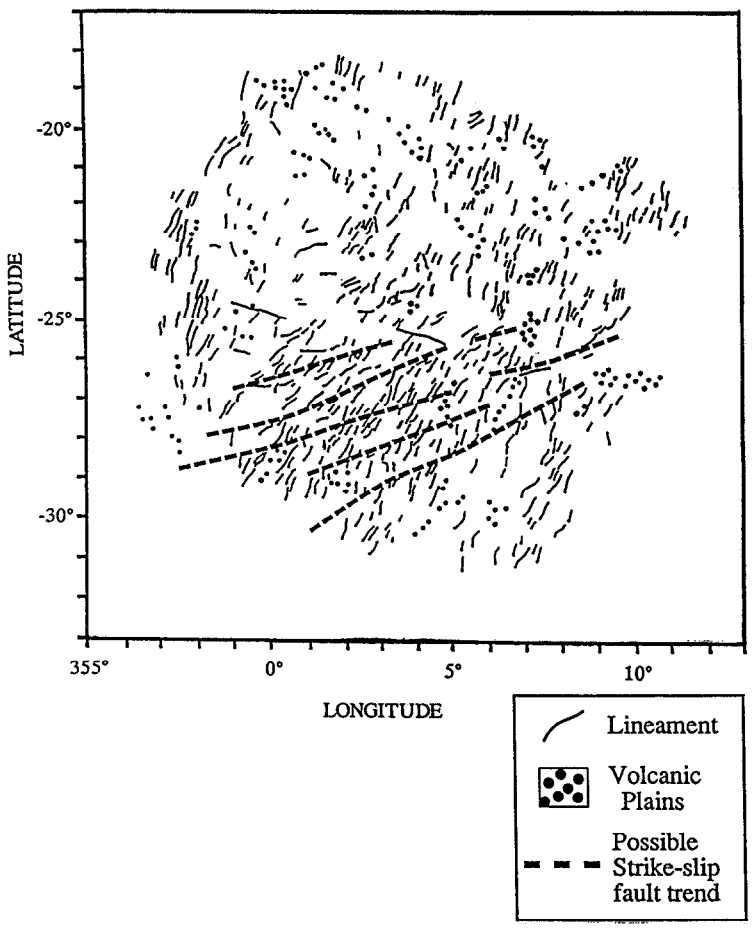

Fig. 4(f). Sketch map showing the location of long linear features within southern and eastern Alpha Regio that disrupt shorter NNE-trending lineaments. The azimuth of these lineaments is about N 70°E and they are interpreted to represent strike-slip faults.

intra-tessera plains would be consistent with basal melting of a thickened crust; and (4) origin of the tessera fabric by horizontal convergence and crustal thickening is also consistent with the "ridge belt"-like nature of the western boundary. Although this model explains many of the features observed at Alpha Regio it cannot fully explain the following: (1) the major N60 °W-trending lineaments and trough in central Alpha; (2) the difference in elevation between northern (about 0.5 km lower) and southern Alpha; (3) the equidimensional outline of the tessera block; (4) the plateau shape of the region and (5) the presence of ovoid-shaped features at Alpha. A second model proposed to explain several of these elements is the sea-floor spreading model in which the ridges and troughs are interpreted to be abyssal hill-like features formed by extension, and the orthogonal central trough is equivalent to a fracture zone (Bindschadler and Head, 1991; Head,

1990). In this case, flooding has obscured other parts of the tessera and subsequent deformation may be responsible for the additional deformation zones (strike slip and the deformation along the western edge). In addition, models of simple extension and gravitational relaxation of a pre-existing topographic high are consistent with many of the observations.

3.3 Ushas, innini and hathor montes

Located at longitude 325° (Figures 1, 2, 5) is a north-south oriented topographic high 2700 × 1200 km in dimension on which occur three circular to elliptical topographic highs. These highs rise to between 2.6 and 3.0 km above the planetary datum (6051.0 km) and correspond to three radar-distinct regions in the Arecibo data. The broad elevated region is similar to areas mapped in the equatorial region as upland rises (Senske, 1990). The northern-most edifice, Ushas Mons, is centered at 25° S, 325°, while 1050 km SSE is Innini Mons (35° S, 330°). Hathor Mons, 600 km southwest of Innini, is located at 40° S, 325°. There is a strong correspondence between distinctive radar-bright features with the local topographic highs (Figure 5a,b). These montes are interpreted to be volcanic in origin on the basis of the following criteria: (1) their isolated, peak-like topography, (2) associated radar-distinct lobes which exhibit a flow-like morphology and radiate away from the central region extending downslope; (3) each edifice has a radar-distinct central region located approximately at the top of the structure that may be the source region of the surrounding deposits; and (4) abundant associated domes and vent-like features.

Ushas Mons is the most well-defined of the three structures; flow units are distinctive and sharp and the lobate nature of the deposits is readily visible. The distribution of deposits interpreted to be volcanic materials at Ushas Mons (Figure 5b, c) is largely controlled by topography. Bright flow units up to 300 km long and 20 to 80 km wide extend radially away and downslope from a radar-dark 200 km wide central area. Overlapping flow units to the north indicate that many eruption events have occurred. The elongation of the high topography appears to have limited flow to the south, producing the distinctive triangular shape. A plot of maximum distance of bright flows from the center of Ushas as a function of azimuth illustrates this asymmetry (Figure 5d). A distinct minimum to the south is observed and it is likely that flows were diverted to the east and west by the steeper regional slopes. Numerous localized vents, domes and cones are found in the region (Figure 5e) (Keddie, 1990). Complex lava flow fields are observed on the northern flanks and base of the volcano and numerous small domes and shields occur there and in the surrounding plains. The generally radar-dark summit region extends to a radius of about 100 km and includes radial zones of brighter material which appear to be flow units emanating from the summit region. In some places, radial spoke-like fractures are observed to cut the flanks and adjacent areas of the edifice; in some cases these are partly obscured by superposed flows. These relations suggest that radial fractures have formed concurrently with the evolution

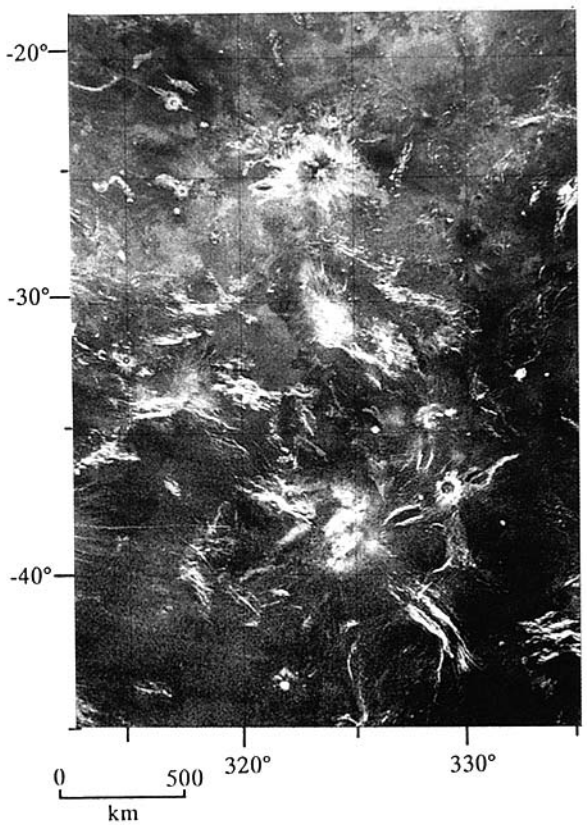

of the volcano. Where the fractures are parallel to the regional topography, as in the case of the zone extending directly to the south of Ushas along the strike of the rise, they are interpreted to be part of a rift zone. Elsewhere, the fractures appear to be linked to the edifice and its immediate surroundings possibly related to radial dike intrusion or deformation through loading and subsidence.

In contrast to Ushas Mons, Innini Mons (Figure 5a–c) is characterized by a bright diffuse central region, approximately 150 km across, which is surrounded by a radar-dark annulus about 80–100 km wide and irregular radar-bright flow-like deposits which extend 200–250 km from the base of the edifice. Bright and dark flow units that extend 600 km from the central region and reach widths of 20 to 120 km occur predominantly downslope to the west and north-east of the structure. The texture at the summit region is mottled and there is a strong suggestion for the presence of several domes and cones. Radial fractures are common and a pair of bright linear features SSW of the edifice at its base appear to be a graben, perhaps part of a flanking rift zone.

At Hathor Mons (Figure 5a–c) the summit region is characterized by an elongate

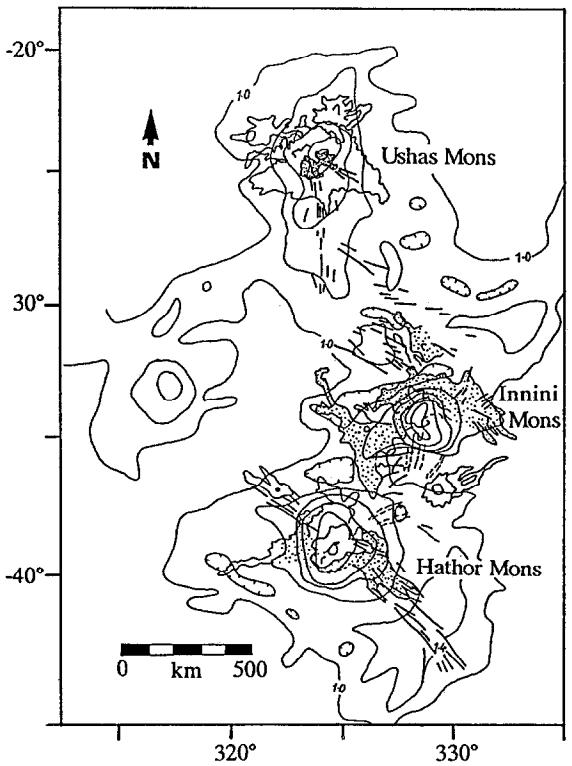

Fig. 5(b).

Fig. 5(a,b). Arecibo radar image (a) and sketch map (b) showing volcanic deposits associated with Ushas, Innini and Hathor Montes overlaid on Pioneer-Venus topography. The volcanic deposits are superposed on local topographic highs (edifices). The increase in the density of stippling corresponds to an increase in radar-darkness (smoothness) of the deposits. Bright lineaments are shown as heavy solid lines. The depressions located to the southwest and north of Hathor and to the northwest of Innini are interpreted as possible flexural features. The topography data is contour at 400m intervals.

area of diffuse alternating bright and dark bands. The central region is bright and contains scarps and numerous small domes. The region is surrounded by a dark annulus about 25 km wide and about 100 km × 175 km at its outer boundary. Distal from this is a relatively brighter annulus averaging about 50–75 km wide that occupies more than three-fourths of the circumference of the edifice; some bright flows extend away from the outer edge of this unit. A radial bright flow unit up to 400 km in length and 20 to 100 km in width appears to originate from a small (approximately 20 km diameter) circular structure in the SW part of the diffuse bright region. The majority of the more distal flows occur to the north and west of the central edifice where the topography drops sharply. The outermost unit is radar-dark and averages 150 km wide with its outermost edge being generally in the vicinity of a low annular topographic rise. The topographic rise may have acted to cause the flows from the shield to pond, producing this boundary. Radial

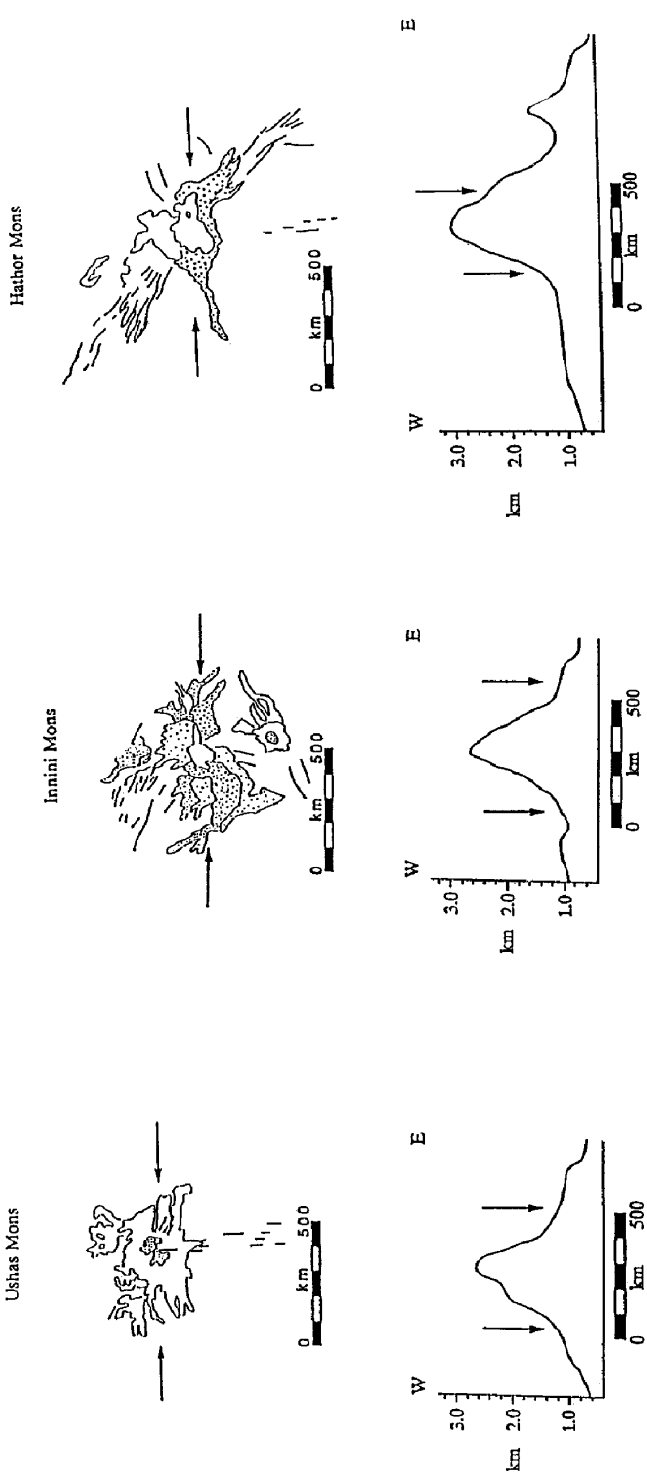

Fig. 5(c). Sketch maps of the volcanic deposits on Ushas, Innini and Hathor Montes along with east-west topographic profiles across the volcanoes. The relative degree of shading corresponds to the degree of radar-brightness. The horizontal arrows on the sketch maps indicate the location of each cross section. The vertical arrows on the profiles mark the maximum extent of deposits along each profile. Deposits are largely confined to the steepest parts of the volcanoes.

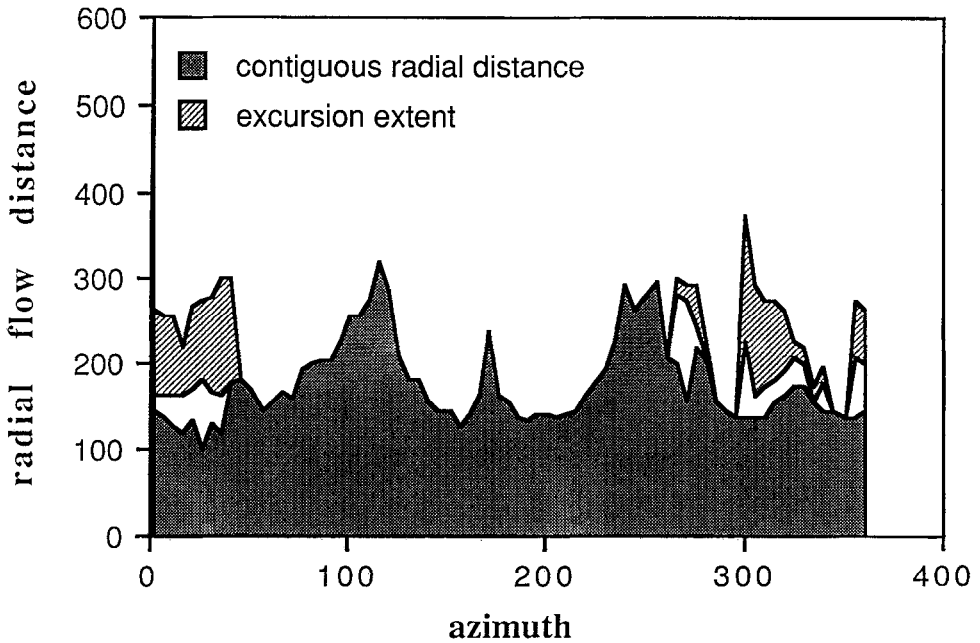

Fig. 5(d). Graph of radial flow distance from the center of Ushas Mons, measured in kilometers, versus azimuth (measured as averages of 10° bins). The maximum values of distance of contiguous deposits at 100° and 230° correspond to the apexes at the base of the "triangular" region of contiguous deposits. The peak at 180° corresponds to a region of deposits that parallels lineaments interpreted to be faults. Excursions are defined as regions of deposits that originate in different azimuth bins and thus are not contiguous with the near-by deposits.

linear features are also present around Hathor, with the greatest concentrations in three linear zones similar to the one located to the south of Innini. These zones begin near the base of the volcano and extend radially to the NW, SE and NE for 200–300 km, eventually dying out or being embayed in the surrounding plains. The topography data (Figure 5b) indicates the presence of depressions interpreted as possible flexural troughs located to the north and west of Innini and to the north and east of Hathor, suggesting that flexural of the lithosphere as a result of the volcanic construction has occurred.

Northeast of Hathor and not directly related to a local topographic high is a 50 km diameter dark circular feature with a bright, 40 to 60 km wide annulus (Figure 5a, b). Bright, somewhat sinuous features up to 250 km long and 20 to 40 km wide radiate away to the north and northeast. These may be lava flows or possibly parts of a tectonic structure (paired rift margins?). Close examination of the image suggests that the bright annulus is superimposed on the flow-like units. It is likely that this is another, less well-developed, volcano associated with the bright lineaments that extend northeast from Hathor.

Cutting across the topographic high and sometimes parallel to its axis are numerous bright lineaments. The trends of these lineaments intersect at the central

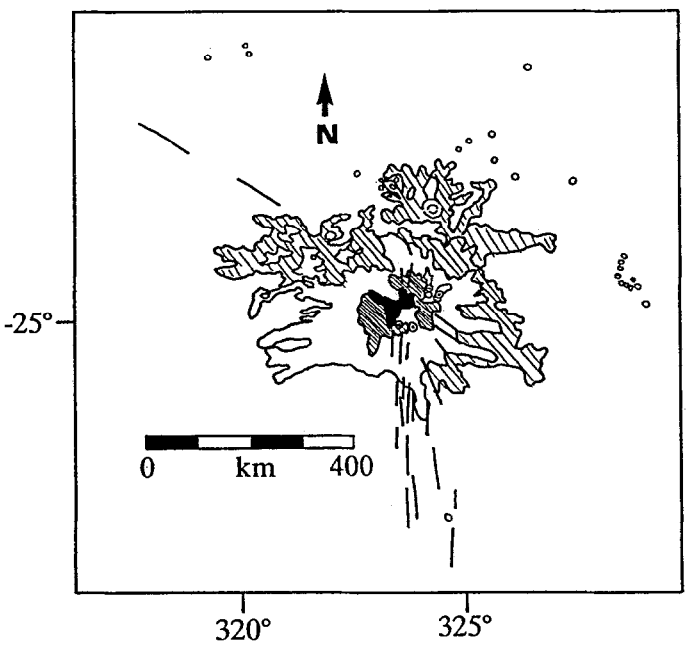

Fig. 5(e). Sketch map of the deposits on Ushas Mons. The degree of shading corresponds to the relative radar brightness of deposits. Overlapping flow units to the north are interpreted as multiple eruption events. Open circles correspond to domes while circles with central dots represent cones. Two cones with short flows are located just to the east of the dark summit region. Radar-bright lineaments interpreted as faults are indicated by the heavy solid lines.

region of all three volcanoes (Figure 5b). This intersection is probably best demonstrated at Hathor Mons where concentrations of lineaments strike NW–SE through the volcano; a second set strikes northeast and a third large array extends to the south. A similar intersection of trends can be observed at Ushas Mons, to the south and southeast. Where the lineaments are arrayed in sub-parallel patterns, such as southeast of Hathor and south of Ushas, they are oriented along local topographic trends. The distribution of flows along these local highs is limited except where there is an association with the lineaments. South of Ushas, the only southward excursion of deposits occurs within and parallel to a bright lineament (the spike within the minimum on Figure 5d). Similarly, flows at Hathor follow the trend of the lineaments both northeast and southwest of the central region. This close association of flows and lineaments suggests the presence of a local low, or trough, indicating that the lineaments may be zones of faulting and rifting, similar to structures at Theia Mons in Beta Regio (Campbell *et al.*, 1984; Campbell *et al.*, 1989).

Although this region is unique in the Arecibo southern hemisphere coverage, several other regions on Venus, including Beta Regio, Bell Regio, Atla Regio and western Eistla Regio, have been interpreted to be regions of thermal uplift and rifting with associated volcanism (Campbell *et al.*, 1989; Janle *et al.*, 1987;

Senske and Head, 1989). Both the superposition of volcanic constructs on the topographic high and the presence of bright lineaments interpreted as faults and scarps, both parallel to the trend of the high and intersecting at the center of these edifices, supports a similar interpretation for this region.

The source of the high topography associated with the rise may be from thermal isostasy, dynamic uplift, or crustal thickening, including volcanic edifice growth. Thermal uplift with superposed volcanism is consistent with the interpretation of this region as a zone of upwelling and, presumably, thinned lithosphere. It is also possible, however, that all of the topography is the result of volcanic construction and thus thickened crust. In this case the three edifices are the most recent centralized sources of volcanism. The relatively limited extent of flow units beyond the local topographic highs (edifices) (Figure 5a–c) suggests that their contribution to the volume of the broad regional topography is limited. However, it is possible that older flows from these edifices and other sources have contributed to the regional topography and subsequently degraded to such a state that they are no longer distinct. The presence of associated radar-bright linear features interpreted to be rifts in the broad rise adjacent to the volcano suggests that some component of uplift and extension has contributed to the development of the regional high. With presently available data, we interpret the broad rise to be primarily due to thermal uplift with associated extension and the topography at each edifice due primarily to volcanic construction, with local contribution to regional topography and resurfacing. The more precise determination of the contribution of constructional volcanism to this region will permit further assessment of its thermal structure.

The method used by Schaber (1988) to calculate lithospheric thicknesses underlying a variety of volcanoes on Venus cannot be employed in this region due to the uncertainty as to the cause of the regional topography. In addition, the presence of possible flexural troughs at Innini Mons and Hathor Mons (Figure 5b) and the implication that flexural loading of the lithosphere as a result of the volcanic construction has occurred, complicates these simple calculations. The low heights of these volcanoes are similar to volcano heights tabulated by Schaber and Kozak (1989), Roberts and Head (1991) and Schaber (1990) for volcanoes in other parts of Venus and are lower and broader than the dimensions of many terrestrial volcanoes. The low elevations could be due to initially low heights or to subsidence and deformation during or after volcano formation.

The volcanoes Ushas, Innini and Hathor are located along a rise generally oriented N–S. Does this trend represent several separate mantle sources or could it represent a chain of volcanoes migrating over a hot spot much like the Hawaiian-Emperor seamount chain? The relative decrease in distinctiveness of the edifice deposits from north to south and the presence of possible flexural moats around Innini and Hathor and not around Ushas, suggests the possibility of an increase in age of the structures southward. The apparent absence of a moat around Ushas and the presence of possible moats around Innini and Hathor would tend to

support this suggestion. However, the irregular spacing of the edifices, the number of adjacent associated edifices and uncertainties in the correlation of radar brightness and age of volcanic flows makes any such suggestions speculative.

The absolute age of volcanism in this region is difficult to ascertain, although crater size-frequency distributions for the entire mapped area (Figure 2c) (Campbell *et al.*, 1990) suggest ages comparable to the relatively young ages for the northern high latitudes (as young as <0.3 Ga, Schaber *et al.*, 1987; or as old as 0.5–1.5 Ga, Basilevsky *et al.*, 1987). Neither the rates of chemical and physical weathering on Venus nor the changes in radar characteristics of lava flows with age are well understood. Examination of the bright haloes around impact craters in Venera 15/16 images (Ivanov *et al.*, 1986) indicates that the roughness of the ejecta blanket and thus radar-brightness, disappears, presumably because of degradation, in about 0.12–0.25 Ga. In Arecibo data (in the Venera overlap region), radar-darkening of once-bright crater haloes is observed to occur more gradually, proceeding in from the outer boundary (Basilevsky *et al.*, 1987). Although different degradation rates would probably apply to a relatively more indurated lava flow, it is possible that a similar darkening of lava flows with age may occur (Kryuchkov and Basilevsky, 1989). The presence of radar-bright flows might then indicate that volcanic activity occurred in the last several hundred million years and that Ushas Mons is the youngest of the three volcanoes. However, radar-dark flows are observed to superpose and thus post-date, bright flows in several places on Venus (Roberts and Head, 1990). Thus the difference in radar brightness of lava flows may be dominated by textural and/or compositional differences rather than age differences. In this region, dark flows have also been observed to superpose bright flows, showing that radar-bright does not necessarily mean 'young'. The very sharp boundaries of the flow units at Ushas Mons is evidence that these deposits are relatively young. Flows at Innini, although less bright, are equally well-defined in places. Embayment of plains material along the base of the rise and possible embayment of linear features that extend from Hathor indicates that at least some plains-forming activity has occurred since or at about the time of edifice volcanism. The linear features that extend east from Themis toward this rise (Figure 2e) appear to cut the surrounding plains, suggesting that they may also be younger than the volcanic rise. Thus, although the volcanoes are probably relatively young geologically, neither their specific age, nor their age relative to other volcanic and tectonic events in this region can be determined confidently with existing data.

3.4. Themis Regio

Themis Regio is a highland region elevated over 3 km above the surrounding plains and is part of a NW trending linear zone extending for over 14,000 km through Atla Regio (Figures 1, 2, 6). A distinctive and unique ovoid chain composed of thirteen ovoids has been mapped in the Themis region (Figure 2d). Two types of multiple ring features were originally described: merged or overlapping

rings (diameters approximately 350 km) and beaded rings (diameters approximately 200 km) (Stofan *et al.*, 1985). Both types of multiple ring features or ovoids are cut by NW-trending radar-bright lineaments, frequently found in pairs spaced about 60 km apart. The ovoids in Themis were interpreted to be endogenic in origin, possibly similar to coronae (Stofan *et al.*, 1985). Nikishin (1986) interpreted the structures as coronae formed over a thermal plume.

The Arecibo images reveal that central Themis is characterized by seven quasi-circular structures ranging from about 250 to 410 km in diameter, with center to center distances of about 400 km (Figure 6). The ovoids are characterized by a discontinuous ring or series of rings, sometimes quite polygonal, made up of numerous radar-bright lineaments similar to the multiple concentric ridges surrounding coronae. The interiors of the features are composed of some combination of radar-dark and mottled radar-bright regions and radar-bright lineaments oriented radially or obliquely to the ovoid. Three of the features have interior radar-bright circular features interpreted to be volcanic edifices; additional volcanic edifices lie to the north and east of the rings (Figure 6b). The central ovoids are connected to smaller (150–250 km diameter) ovoids to the northwest by radar-bright lineaments that both cut and terminate at the ovoids. We interpret the lineaments in Themis to be extensional in origin on the basis of their association with volcanic features, their alignment along the axis of high topography and their similarities to extensional features elsewhere on Venus. Cross-cutting relationships indicate that the ovoids and extensional deformation occurred concurrently. On the basis of restoration of ovoid structures that appear to be split and separated, Campbell *et al.* (1991) have estimated the amount of extension in this region to be in the 10–15 % range.

The Themis ovoids are similar to coronae in size, association with relatively raised topography and annulae of concentric lineaments. However, the Themis ovoids are dissimilar in the extreme polygonality of some of the features, the strong association with tectonic lineaments and their chain-like nature. Coronae in the northern hemisphere of Venus tend to occur as isolated features in the plains or in clusters spaced over 600 km apart The Themis features resemble a group of corona-like structures south of Ishtar Terra in Sedna Planitia (Stofan *et al.*, 1987) interpreted by Raitala and Tormanen (1989) as a possible hotspot chain. However, the features in Sedna have little or no topographic relief and have ambiguous age relationships. The Themis Regio ovoids are also similar to ovoids within the Beta-Eistla Deformation zone (Stofan *et al.*, 1990a), which is characterized by smaller ovoids (80–240 km across) connected by radar-bright lineaments and associated with lower topography.

The similarities of the Themis ovoids to coronae suggests that they may be formed by similar processes (rising thermal anomalies; Stofan *et al.*, 1990b), but their chain-like appearance and close association with lineaments interpreted to be extensional in origin indicate a more complex origin. We suggest three possible models of formation for the ovoid chain in Themis Regio:

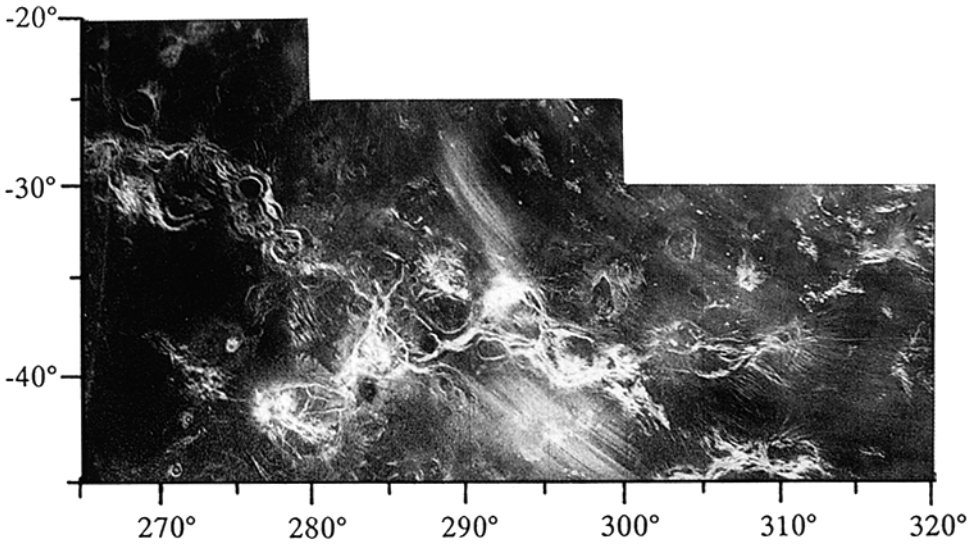

(a)

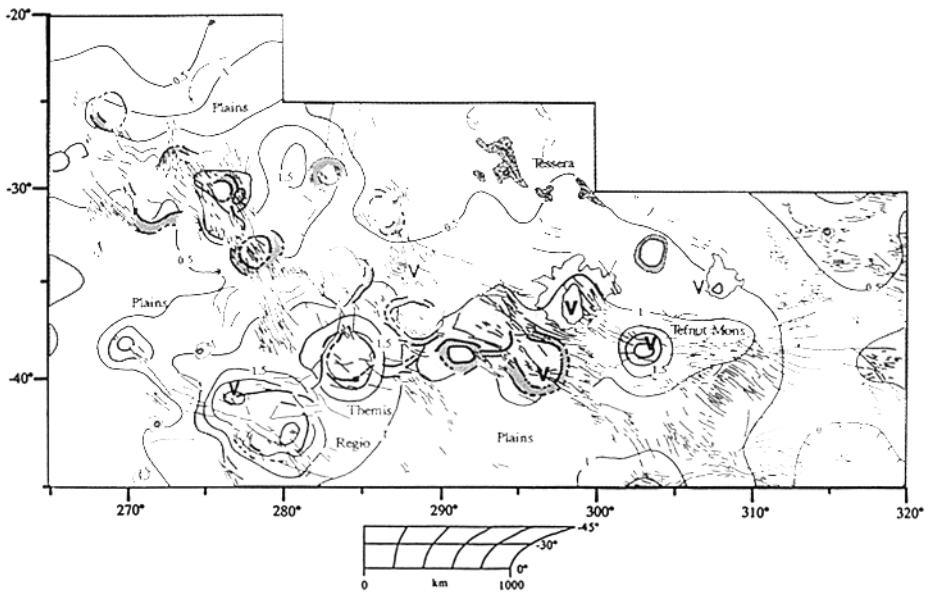

(b)

Fig. 6. (a) Arecibo radar image showing the chain of ovoids in Themis Regio. The bright wispy features are artifacts resulting from the technique by which that data were acquired. (b) Sketch map of Themis Regio and Pioneer Venus topography contoured at 500 m intervals. Central Themis rises to an elevation of 2.5 km and is characterized by two topographically distinct arcuate to circular features. The heavy bold arcs, shaded arcs and circular features indicate the location of ovoids. Features labelled "V" indicate the location of centers of volcanism. Lineaments interpreted as faults and fractures are indicated by the thin solid lines.

(1) Hot spot chain: The ovoids in Themis may be formed by a thermal plume beneath a moving plate. The predominance of volcanic structures, such as Tefnut Mons, in the eastern portion of the ovoid chain would suggest that the plate would be moving west-northwest. If this were true, one would expect the topography of the features to decrease and the age of the features to increase in the northwest. However, there is no clear trend in topography in this direction as seen at terrestrial hotspot chains. The highest topography actually lies just to the southwest of the center of the chain at one of the ovoids. In addition, there is no clear trend in age of the features. The central ovoids do not overlap in any discernible pattern, nor is there any distinct trend in volcanic activity, other than the fact that there are more identifiable volcanic edifices on the eastern half of the chain. At this time, no strong evidence can be found to support the interpretation of the ovoid chain as a hotspot chain.

(2) Zone of extension accompanied by upwelling: The Themis Regio ovoid chain is part of a linear zone that extends for thousands of kilometers to the northwest into Atla Regio. The smaller ovoid chain is on a trend that is aligned with Parga Chasma, a 0.5 km deep trough with raised rims that joins up with Atla. The predominance of lineaments interpreted to be extensional in origin indicates that the ovoid chain may lie along a major zone of extension extending from Themis Regio to Atla Regio. The ovoids are interpreted to form from diapiric rise of magma along this zone of extension. The central high topography of Themis and the central group of ovoids may be caused by the intersection of this zone of extension with a thermal plume, causing multiple upwellings of material to form the large ovoids.

(3) Zone of active crustal spreading: The Themis Regio ovoid chain may be a zone of active crustal production and spreading, accompanied by magma upwelling or underlain by thermal plumes to form the ovoids. However, no evidence of transform faulting and limited evidence for split and separated features are seen at Themis. The eastern termination of the chain of ovoids is characterized by a long linear radar-bright feature that extends beyond a splayed-out group of lineaments (Figure 6). The relation between features in this area suggests that the Themis ovoid chain may lie along a propagating rift.

3.5. Navka-Guinevere planitiae

The plains of Navka and Guinevere (Figure 1) consist primarily of bright and mottled plains, a southern extension of mottled plains mapped in the equatorial region to about 40° N (Senske, 1990; Senske *et al.*, 1991). The mottled plains contain evidence for multiple flow units, some of which are associated with large edifices such as Ushas Mons and others of which are probably related to individual volcanic domes and shields as previously observed in central Guinevere Planitia (Campbell *et al.*, 1989).

Small domes and shields are the smallest resolvable features with distinguishing

characteristics and based on Venera 15/16 data appear to be the most numerous volcanologic feature on Venus at this resolution (Aubele and Slyuta, 1990). Domes have previously been defined and identified on the basis of their positive topographic relief and generally circular planimetric outlines (diameters in the range of 2–20 km and slopes of $\leq 10°$). Associated characteristics include summit pits and radar bright or dark surfaces. On the basis of their morphology, terrain and geologic associations (Aubele and Slyuta, 1990) and theoretical analysis of Venus eruption conditions (Head and Wilson, 1986), the domes are interpreted to be shield volcanoes constructed from dominantly effusive eruptions. Within the Venera image area, domes commonly occur in spatial association with coronae, arachnoids, intermediate sized volcanoes, large volcanic centers and calderas.

For most of the range of incidence angles that occur in the Arecibo coverage, the radar system is sensitive to changes in surface roughness, therefore radar bright features are interpreted to exhibit roughness that varies at the wavelength of the radar, although it is increasingly sensitive to changes in topographic slope near the equator. For this reason, domes are easily recognized on mottled plains (Figure 2d); areas where the incidence angle is $\leq$ the 40° iso-incidence contour line (Figure 7), with domes most easily recognized in the area $\leq$ the 30° iso-incidence contour. A number of bright spots that are visible in the area $\geq 40°$ iso-incidence contour may represent small domes, but identification is difficult since small radar bright spots on the image may be caused by a variety of properties and processes. The general lack of visible domes in the southern part of the area is probably directly attributable to the effect of variable incidence angle; however, there may also be a real decrease in dome number to the south in the region of lineament belts in Lavinia Planitia. If these lineaments are interpreted to be structures similar to ridge belts, then the dome density and number of domes may decrease near the belts in a manner similar to the general decrease in dome number in regions of ridge belts in the areas imaged by Venera (Slyuta *et al.*, 1988; Slyuta and Kreslavsky, 1990).

The domes identified in the area bounded by the 30° iso-incidence line are relatively large (intermediate-sized edifices based on Venera classification; Slyuta and Kreslavsky, 1990) and occur as single edifices. In general, only domes ≥ 10 km in diameter are visible. The most common appearance of domes is as a bright spot or a diffuse bright spot, although some domes in the area bounded by the 20° iso-incidence line appear to show radar bright and dark topographic flanks. Clusters of smaller domes occur spatially in association with the large edifices, particularly Tefnut Mons and Ushas Mons along with the interior of some ovoids. While Hathor Mons and Innini Mons also would be expected to have associated clusters of domes, very few domes can be identified near these edifices. Either the domes are not present, which would be unusual based on analysis of Venera images of the spatial association of larger volcanoes and clusters of domes (Slyuta, 1990; Aubele and Slyuta, 1990), or they are not visible due to lack of significant variation

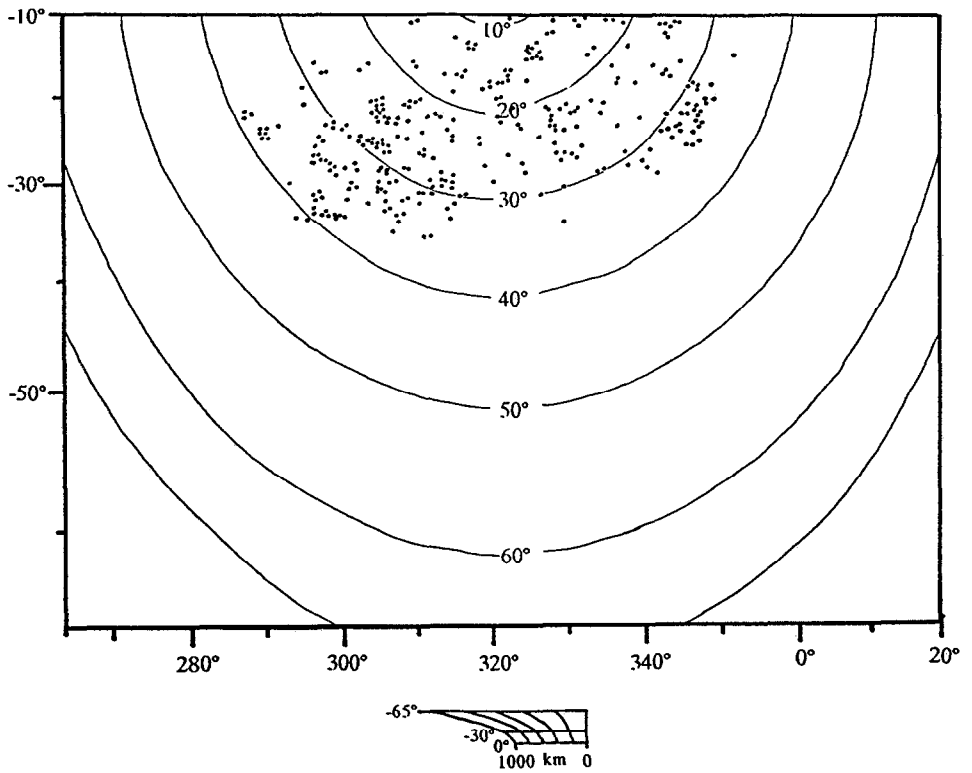

Fig. 7. Map showing the distribution of domes in relation to lines of constant incidence angle. Domes are most easily recognized at incidence angles less than 30° where the radar is sensitive to variations in surface topography.

of the domes in roughness from the surrounding plains. There is also a lack of identifiable domes near Phoebe Regio, even in the area $\leq 40°$ iso-incidence contour (Figure 7).

Radar bright or dark patches are visible around some of the individual domes that occur $\leq 30°$ iso-incidence line. In most cases, these patches are halos or aureoles that appear to surround or partially surround the dome to a distance of 1 to 2 dome diameters. In one case, a finger-like bright feature is interpreted as a flow associated with a dome. No summit pits are visible, but at this scale they would probably be difficult to detect. The presence of significant radar signal return from some domes at incidence angles up to 40° suggests the presence of flanking material that possess surface properties that promote radar backscatter such as high surface roughness. However, the range of backscatter of domes and the range of backscatter of the plains in which they are associated seems to be generally comparable indicating that the domes and their immediate surroundings may be composed of the same material and that the surface roughness may be

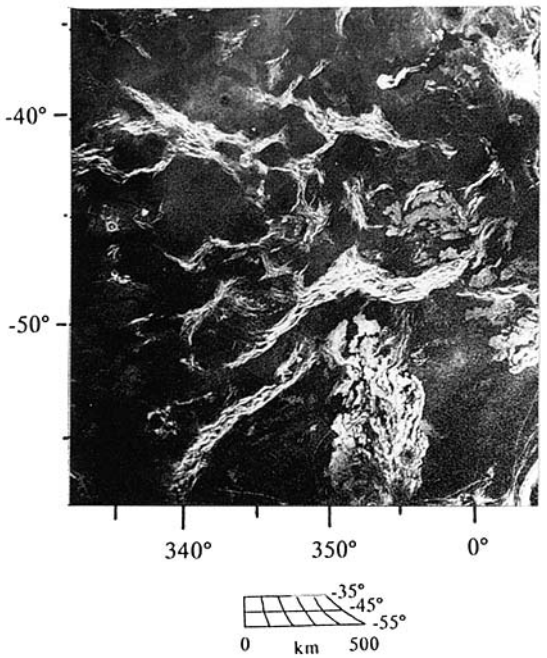

Fig. 8(a). Arecibo radar image of linear deformation zones in Lavinia Planitia.

caused by the presence of variable textured or degraded surfaces rather than by a different material.

3.6. Lavinia planitia

Lavinia Planitia is a kidney-shaped depression occupying about 5×10^6 km^2 and surrounded by the volcanic edifices Ushas Mons, Innini Mons and Hathor Mons, an arch separating Lavinia from southern Guinevere to the north, Alpha Regio to the northeast, the edge of Lada Terra to the east and south and an arch between Lada and Themis, separating southwestern Lavinia from Helen Planitia. The area of Lavinia is about five times larger than the lunar Mare Imbrium and the deepest parts of the basin (41° S, 350°) are at an elevation less than 1.0 km below mpr, the lowest point in the mapped area. Located within Lavinia are lineament belts and a variety of plains units (Figure 2d) with bright plains and digitate plains dominating the eastern half and dark plains dominating the western half. These units lie in marked contrast to the stippled plains of Helen Planitia.

3.7. Linear deformation belts

Linear deformation belts in Lavinia Planitia (Figure 2d, e) are zones 75–250 km wide and 200 to 2000 km long containing radar bright lineaments spaced 5–40 km apart (Figure 8a, b). The incidence angle for which Lavinia is observed ranges from 35° to 60°; it is therefore not possible to determine whether or not the

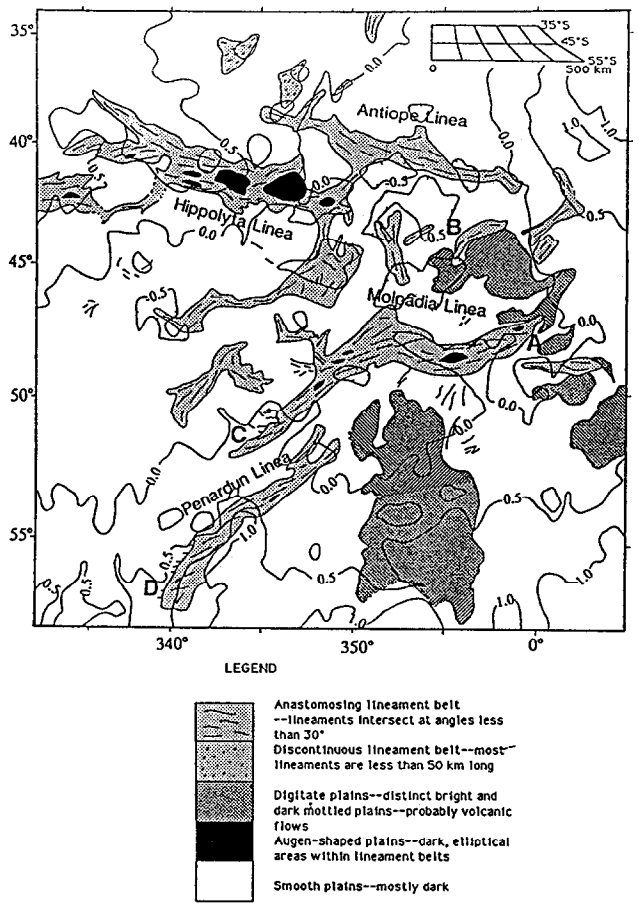

Fig. 8(b). Sketch map of lineament belts in Lavinia with Pioneer Venus topography superposed. Contour intervals are every 500 m and are referenced to a planetary radius of 6051.0 km. The belts corresponding to Hippolyta Linea, Antiope Linea, Molpadia Linea and Penardun Linea are elevated between several hundred meters to 1.0 km above the surrounding plains.

individual radar bright lineaments correspond to ridges, troughs, or scarps. The separation distance between lineament zones ranges from about 150–750 km with the most common spacing being 200–300 km apart (Figure 8c). The cumulative length of all the linear deformation zones in Lavinia is 11,900 km (Figure 8d). Most of the lineament zones are located on local topographic highs (Figure 8b) and many are in close proximity to the distal portions of the relatively recent flows of the digitate plains. Augen-shaped regions of plains up to 120 km wide and 220 km long are common within the lineament belts (Figure 8a, b) and are similar to those seen in the ridge belts in the northern hemisphere, especially in the fan to the east of Atalanta Planitia (Frank and Head, 1990b; Sukhanov and Pronin, 1989). Smaller, oval to cigar-shaped, or linear patches of radar-dark material, interpreted as plains of volcanic origin which are similar to the regional units

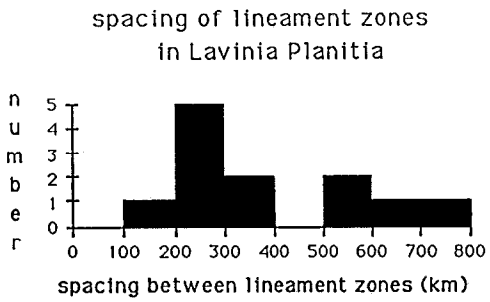

(c)

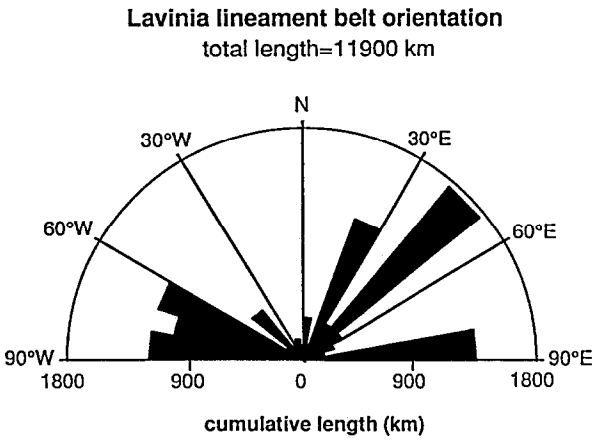

(d)

Fig. 8. (c) Plot of frequency versus spacing between lineament zones; the dominant spacing is between 200 and 300 km. (d) Rose diagram showing the variation in orientation of the lineament belts.

within Lavinia, are also found within the lineament belts (Figure 8a, b). Although the general appearance of the lineament belts locally appears to be anastomosing, several distinctive trends occur, including one centered on N 20–50° E, one E–W and a less distinct trend oriented N 60–70° W (Figure 8d). The first and third trends are somewhat similar to those seen in Alpha Regio to the northeast (Figure 4).

The most prominent lineament zones are located in central Lavinia Planitia (Figure 8a, b). Hippolyta Linea and Antiope Linea (centered on 41° S) are broad (100–200 km in width), radar-bright and rise locally from 0.5 to 1 km above the adjacent lowland plains (Figure 8b). The second prominent lineament zone, Molpadia Linea (about 48° S), is also radar bright and topographically high, as is Penardun Linea. There is a suggestion of topographic relief associated with the other lineament zones (variations in contours and local high points), but they are

not wide enough to be distinguished at the resolution of the PV data. Additional evidence for the topographic prominence of the linear deformation zones comes from apparent embayment of plains surrounding the zones. In many places, such as at the NE end of Molpadia Linea (Figure 8b; A,B), flow units of bright plains (parts of the digitate plains) bifurcate and flow around the lineament zones. In these areas, a few km of radar dark plains are visible between the lineament zone and the bright flows. On the assumption that the flow units are seeking the lowest topographic level, we interpret this to mean that the topography adjacent to the lineament zone is tilted up toward the lineament belt.

In the central region, the most common spacing between adjacent lineament zones is 200–300 km (Figure 8c). Visually, the orientation of the lineament zones is dominated by the NE trending southern (48° S) lineament zone and the WNW trending northern (41° S) lineament zone, but the orientation of the shorter, less regular lineament zones is also evident (Figure 8d). The north-south trending zone at 44° S, 347–352° illustrates one of the variations in trend of these smaller lineament zones. The prominent lineament zones along the northern boundary of this region have distinctly asymmetric patterns; the north side is brighter (rougher) than the south side. If this asymmetry in roughness is due to more intense deformation in the roughest area, then it may be similar to the asymmetry in style of deformation observed in some of the ridge belts east of Atalanta Planitia in the Venera coverage (Frank and Head, 1990b).

The boundaries between lineament zones and the surrounding smooth plains in directions parallel to the strike of the zones are usually abrupt and lineaments are often parallel to the boundaries. However, in some cases (C and D on Figure 8b) lineaments are at angles up to 50° from the trend of the boundary, suggesting that the lineament zones were faulted and embayed by volcanic plains subsequent to the tectonic deformation. In addition, some of the smaller patches of lineament zones are surrounded by narrow collars of dark plains, which in turn are surrounded by deposits of bright plains. These relationships suggest that the linear deformation zone was formed, adjacent dark plains were uptilted during or after the deformation and subsequent bright plains were emplaced in the lows. This is a relationship that is also observed in lunar mare ridges (Watters, 1988) where it is seen that compressional deformation forms the ridges and tilts the adjacent maria and then these linear belts act as kipukas during further flooding of the lunar maria (Pieters *et al.*, 1980). These embayment relationships strongly suggest that the tectonism forming the lineament zones is closely linked to and overlapping in time with the plains volcanism. In addition, in several places, one or two bright lineaments of the lineament zone extend beyond the main structure, apparently cutting adjacent bright younger flow units (Figure 8b; A). In other places numerous bright lineaments (with a density lower than the density of the lineament belt itself) sweep out beyond the lineament zone into the surrounding plains (Figure 8b; C,D). These relationships suggest that some of the deformation of the lineament belts may actually postdate the emplacement of the adjacent plains, or that the lineament zones were faulted and the edges covered by plains.

Many of the features listed above are also common in the ridge belts east of Atalanta Planitia and imaged by the Venera 15/16 spacecraft (Sukhanov *et al.*, 1989; Frank and Head, 1990b). The following are observed in both regions: (1) the most prominent lineated zones are on local topographic highs; (2) there are two wavelengths of spacing; spacing is regular on a 5–40 km scale (lineaments) and a hundreds of km scale (lineated zones); (3) linear deformation features are arrayed in a fan-shaped pattern (apex pointing N in the area east of Atalanta and E in Lavinia); (4) both lineaments and lineated zones are sinuous and anastomosing; (5) lineated zones have distinct boundaries with plains; (6) augen-shaped plains are abundant; and (7) individual lineated zones are asymmetric. The characteristic spacing of ridge belts in Atalanta Planitia have been used to infer a structure for the crust and upper mantle for that part of Venus (Zuber, 1987; Zuber and Parmentier, 1990). When compared with Atalanta, the dominant wavelengths of deformation in Lavinia are found to be similar in both regions. Application of the model proposed by Zuber (1987) suggests a structure for Lavinia in which strong crustal and mantle layers are separated by a weak lower crust. On the basis of this model and the similarity in wavelengths of deformation between the two regions, it is suggested that the crustal layer in Lavinia may have a thickness similar to that in Atalanta (between 5 and 30 km) (Zuber, 1987).

On the basis of the following evidence, we interpret the lineament belts in Lavinia to be predominantly of compressional origin: (1) local positive topography, (2) occurrence in regional low-lying areas (in contrast to linear highs), (3) lack of local negative topography that might be associated with rifting, (4) lack of evidence for widespread extension (e.g., split and separated features), (5) contrast in morphology to other linear deformation zones in the mapped region interpreted to be of extensional origin, (6) lack of evidence for associated large-scale volcanic sources, (7) similarity to ridge belts in the northern hemisphere viewed with lower incidence angle which have been interpreted by Frank and Head (1990a) to be of compressional origin.

It is difficult to determine if any of the lineament belt trends show cross-cutting relationships and any evidence for a sequence of events for belt formation. At one location, a NE-trending belt segment appears to crosscut a WNW trending segment (Figure 8b; D), but these two directions are normal to and parallel to illumination directions respectively and thus are not completely independent of look-direction enhancements. The lineament belts within Lavinia are often parallel to tectonic trends in the adjacent terrains (Lada Terra, etc.) but no firm relationships have been established between them. Thus, with available data, we have been unable to distinguish whether the lineament belts within Lavinia formed concurrently, or whether there is a sequence to their formation.

3.8. Digitate plains

Unusual, extensive, isolated regions of radar-bright lava flows have been mapped in Lavinia Planitia as digitate plains (Figures 2d; 9a, b). The largest of the lava complexes is centered at 354°, 54° S and extends approximately 940 km N–S and

400 km E–W. The complex is located near the southern boundary of Lavinia Planitia and is surrounded by radar-dark plains. Rough-textured, radar-bright linear deformation zones border the complex to the north and south. Molpadia Linea borders the complex to the north and is interpreted to be primarily compressional in origin as discussed previously. To the south, the complex is bordered by the lineament zone at the northern edge of Lada Terra (Figures 1, 2d), interpreted to be of extensional origin. The largest lava complex appears to be closely linked to and largely superposed on, the southern lineament zone and terminates against Molpadia Linea and adjacent lineament zones in the north.

The complex is characterized by very long, lobate, radar-bright flow units many of which may extend up to the full 940 km length of the complex (Figure 9b). The widths of individual flow units vary from 10 up to 140 km (particularly where they appear to pond). The three brightest flow units (easternmost deposits; Figure 9) each average 20 km in width and range in total length from 470 to 640 km. The flow units are lobate, tend to pond in their northern extremities and are diffuse and obscured near the linear deformation zone to the south. Two possible volcanic edifices have been identified as sources for many of the flows and several other circular to arcuate features have been mapped within this southern part of the complex (Figure 9c). On the basis of these characteristics and regional topography (Figure 1) we conclude that lavas in the complex originate in the vicinity of the linear deformation zone and have flowed downhill primarily to the north, ponding in the lowest part of Lavinia Planitia, just to the south of Molpadia Linea.

The two most notable features that appear to be sources for these flows are located at the southern end of the complex, in the gap along the strike of the lineament belt. The westernmost dark circular area (Figure 9c; "a") is about 145 km in diameter, is on a local high (rising 0.5 to 1 km), has an oval summit depression about 20×33 km that we interpret to be a caldera, is surrounded by diffuse brighter deposits which embay parts of the linear deformation zone, a suspected impact crater to the SE and extends for about 320 km to the southeast. The second vent (Figure 9c; "b") is located on the north slope of the lineament zone at a radar-dark circular feature about 140 km in diameter and this structure appears to be the source for the easternmost flow units (Figure 9c). It is located at a V-shaped apex from which the flows appear to originate. A third possible vent (about 60 km in longest dimension) in this area is located about 115 km NE of the first vent (Figure 9c; "c"). Flows emanating from the western vent appear to be arrayed somewhat radially in the 200–300 km surrounding the vent, but those on the NE flank turn northward and flow down the regional slope into the basin. Flows emanating from the eastern vent extend directly downslope into the basin, except for a local embayment of the linear deformation zone to the west. Flows from the eastern vent appear to superpose those from the western vent, indicating a younger age (Figure 9c). In addition, stratigraphic relationships have been identified within flows originating from the eastern vent (Figure 9c); the three brightest flows appear to comprise the youngest units from this source. Both

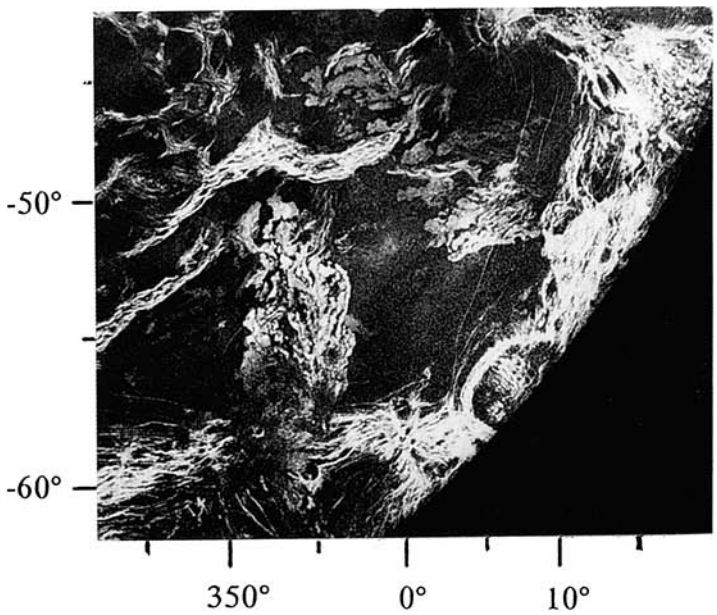

(a)

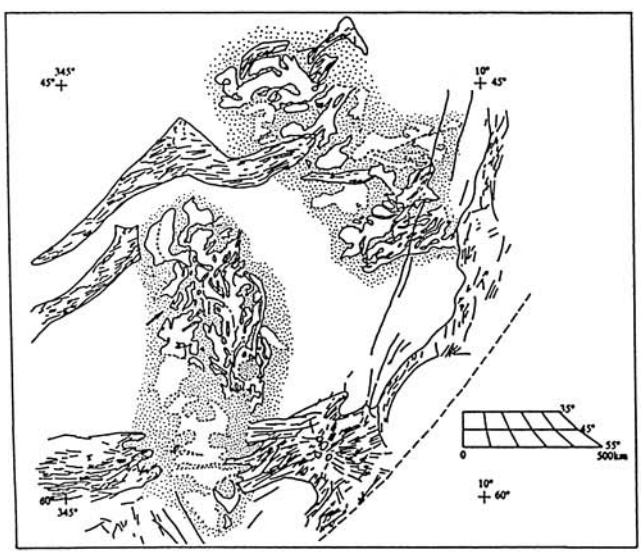

(b)

Fig. 9(a). Arecibo radar image of digitate plains and linear deformation zones in Lavinia Planitia. (b) Sketch map illustrating units of digitate plains and trends of adjacent lineament belts. Bright flow boundaries are outlined and dashed where uncertain. Underlying dark plains and dark flows are dotted; the arrow indicates the location of a relatively young dark flow.

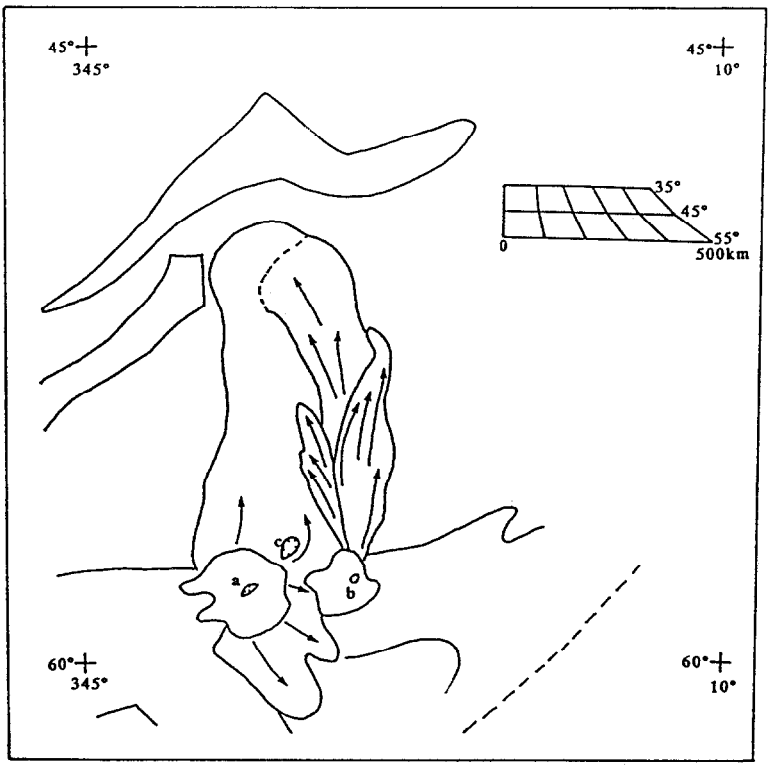

(c)

Fig. 9(c). Schematic map showing major flow units (arrows indicate the general direction of flows) and possible source areas ("a", "b", "c").

sets of flows extend for several hundred km northward into the basin until they reach an apparent structural discontinuity and their flow is disrupted or diverted. This discontinuity (Figure 9d; arrow) is oriented NE–SW and is parallel to the strike of the lineament belts to the north. In this region, the flows change course, terminate or become more lobate as they apparently respond to local topographic highs and lows. Another characteristic of the southern source region is the presence of a ghost-like ring structure made up of somewhat concentric arcs (Figure 9d; dotted circle) about 300 km in diameter; in the same range as the corona-like features located elsewhere along the same lineament belt and may be a similar feature, but heavily modified by volcanism.

A distinctive aspect of this deposit and the other digitate flow occurrences is the diffuse nature of the flow units in the proximal upslope regions compared to their distal bright deposits. The diffuse nature of the units in the region of source vents could be due to: (1) changes in the surface roughness as a function of distance from the vent; in this case, smoother flow surfaces (pahoehoe-like?) could

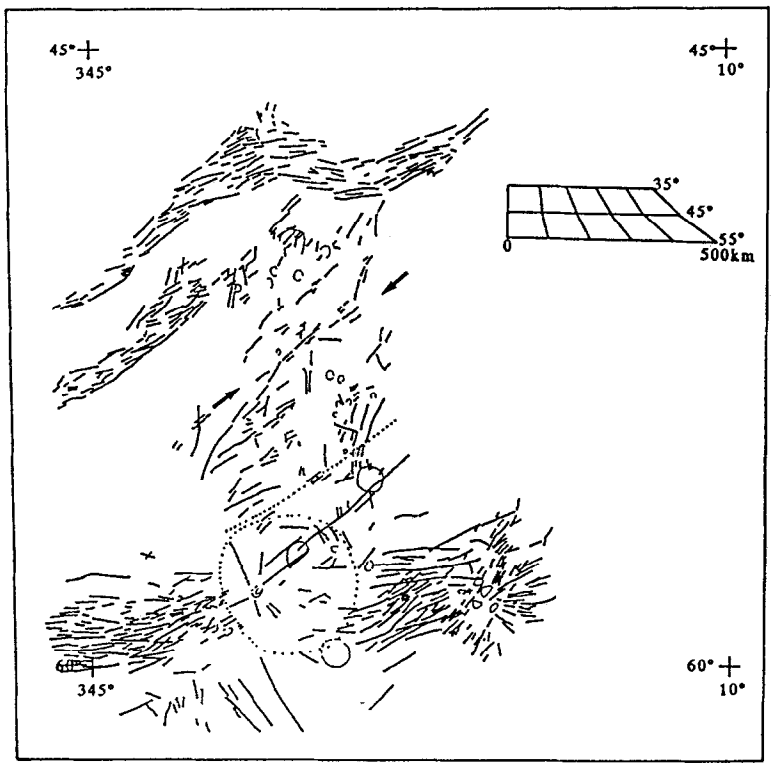

(d)

Fig. 9(d). Sketch map of major structural elements and circular features within the lava complex and adjacent lineament belts. Arrows indicate the trend of a structural discontinuity that disrupts the distal region of the flow units. The dotted circle outlines a faint corona-like feature.

dominate near the vent and not be readily distinguishable from one another, producing diffuse-appearing deposits and then evolve to rougher-surfaced radar-bright units (aa-like?) as they continued to flow and cool; or (2) deposits that have masked an initial heterogeneity and brightness; these could be due to later-stage deposits associated with the same sources that overlie the brighter lobate deposits to the north. Shorter, younger flows with a different surface texture could be a candidate for such deposits. Pyroclastic deposits of regional nature, although not favored in the Venus environment (Head and Wilson, 1986), could also be a candidate for such an origin. However, the diffuseness extends further in a N–S direction (along the strike of the flows) than in an E–W direction (into the adjacent lineament zone), leading us to consider this possibility less likely.

In general, this and the other digitate plains complexes consist of bright flows superposed on dark plains. However, in one case in the NW portion of the larger complex (Figure 9b; arrow) there is an isolated patch of a bright flow unit that

appears to be a kipuka of older bright flows surrounded by younger lobate dark flows. Kryuchkov and Basilevsky (1989) compared radar-bright flows to the bright haloes observed around fresh impact craters and suggested that bright flows represent the youngest (<200 m.y.) volcanic activity on the planet. Although stratigraphic evidence indicates that these bright flows are some of the youngest units in the area, observations elsewhere (Campbell *et al.*, 1989; Roberts and Head, 1990) indicate that radar dark flows are locally found superposed on radar bright flows in data from the same radar system. This, combined with the fact that variations in surface brightness are seen with range along these flows, suggest that it is unlikely that flow-brightness variations are solely the result of aging processes; variations in parameters such as lava rheology and thermal structure also need to be considered.

Numerous lineations have been mapped within the complex (Figure 9d) may represent ridges, scarps, grooves or deposit contacts and appear to be structural in origin. To the south, the trends are curvilinear and appear generally concentric to the dark circular deposits in the proximal upslope region of the complex; this may be related to the ghost corona-like structure. A throughgoing dark lineament is observed trending NE across the southern part of the feature, cutting through the western and central vents. This trend is an extension of the bisector of the chevron structural unit mapped to the south (Figure 2e). Another parallel, but less distinct dark lineament is observed about 130 km to the north (Figure 9d; dotted line). To the east and within the brightest flow unit, the lineations are closely spaced, long and subparallel to one another and individual flows within the unit. Locally, they appear to have exerted structural control on the flow direction of deposits in this unit. To the north, lineations are more chaotically distributed in a complex, intersecting pattern that is similar to and, in some cases, can be directly traced to the arrangement of lineations in neighboring lineament belts. Flows to the north have often flowed between these lineations, apparently following lows between ridges. The deposits of the southern complex clearly flow around and abut the linear deformation belts in the north and also overlie portions of the lineament belt to the south and are therefore younger than the deformation associated with these zones.

Three additional lava complexes are centered at approximately 6°, 51° S; 5°, 47° S; 0°, 45° S. They are located at the eastern edge of Lavinia Planitia and flow downslope in westerly directions. Although less extensive in total length, they are similar in general appearance to the lava complex discussed above. Individual flow units within each complex are less linear and more polygonal than those of the larger complex although the range of lengths and widths of individual flow units is comparable. No obvious source vents are observed within the smaller complexes and few circular features are mapped. The bright flow units become obscured toward their apparent sources in the adjacent lineament belt (Figure 9a, b). This relationship is similar to the one observed in the deposit to the south, again suggesting the possibility of changes in flow surface roughness as a function of

distance, or later-stage deposits with different radar characteristics. Flow units within these complexes appear to have abutted and embayed the lineament belts in central Lavinia Planitia (particularly Molpadia Linea), suggesting a younger age for the flows. Two of the complexes may be crosscut by two 1350 km long lineaments trending ~N–S that are part of the zone of deformation bordering Lavinia Planitia to the east (Figure 2e), but the detailed relationships are ambiguous. In any case, it appears that the digitate flow units of these lava complexes have emanated from the linear deformation belt bordering Lavinia Planitia to the south and east, in one case postdating the belt and that they have flowed down into Lavinia, flooding and flowing around the linear deformation belts on the floor of Lavinia, largely postdating them.

In summary, the lava complexes of Lavinia Planitia are dominated by radar-bright lobate flows originating in the surrounding linear deformation belts and superposed on the plains of Lavinia Planitia. Edifices or source vents are only discernible in the southern occurrence; other sources may be obscured by subsequent deformation along the linear deformation zone. This is consistent with the observation that each complex appears to terminate upslope near the boundary of a linear deformation zone and the fact that if deformation continued along the southern complex source region, they too would be modified and likely obscured. The localization and brightness of the deposits relative to the majority of Lavinia Planitia may be related to a local source of numerous, younger, rougher flows. The brightness of the flows may be partly linked to intrinsically greater reflectivity or roughness (which would be linked to magma rheology, composition and thermal structure). The lava complexes are isolated within Lavinia Planitia; no similar occurrences are observed elsewhere in the Arecibo data except perhaps to the southeast of Lakshmi Planum in the northern hemisphere (~350°, 55° N) (Stofan *et al.*, 1987). The factors controlling the formation and evolution of the lava complexes are most likely related to the tectonic environment of the linear deformation belt at their source regions.

3.9. Helen planitia

Helen Planitia (Figure 1) is a lowland located between Lada Terra and Themis Regio and extending to the west into a region unmapped by Arecibo. Helen also appears to extend to the south of the Lada lineament belt to about 335° and 79° S. In contrast to the other regions of lowland plains, Helen has no well developed structures or textures and is characterized by a few poorly defined ghost structures and lineaments (Figure 2d, e). In addition, Helen and its vicinity are dominated by the 'salt and pepper'-like stippled plains, which appear relatively smooth at radar wavelengths and have intermediate to high reflectivity values in PV data (Head *et al.*, 1985). The lack of distinctive features and the homogeneous nature of the plains could be attributed to a greater age (lack of recent activity and degradation of older features) but the distribution of craters is not markedly different here than elsewhere. In addition, Lakshmi Planum appears relatively

homogeneous in Arecibo images although abundant detail is observed in Venera 15–16 images (Pronin *et al.*, 1986; Roberts and Head, 1990). Thus, viewing geometry and radar system characteristics may also be factors in the interpretation of Helen Planitia.

3.10. Lada terra

Lada Terra is a southern high latitude upland or highland region first identified in PV topography (Pettengill *et al.*, 1980; Masursky *et al.*, 1980). It is located south of an arcuate line beginning at 65° S, 280°, extending along the southern edge of Lavinia Planitia up to Alpha Regio and across to the vicinity of 30° S, 40° and over to about 65° S, 130° (Figure 2c). The topography south of about 65° S is not known and thus the total extent and elevation distribution of Lada is unknown. In areas covered by PV, the topography averages about 0.5–1.5 km above mpr, with occasional peaks rising over 2 km. Although the topography is lower on the average than the northern high latitude highlands (Ishtar Terra), there has been much speculation on the possible similarities and differences between the two high latitude highlands. The Arecibo images reveal some of the characteristics of western Lada Terra for the first time.

Lada Terra is characterized by four major units in the mapped region (Figure 2d,e): (1) a linear deformation zone extending from Helen Planitia eastward along the northern edge of Lada and curving NNE toward Alpha Regio; (2) ovoids, some of which are interpreted as coronae, located along the lineament belt extending up to Alpha Regio (Campbell *et al.*, 1991); (3) a tessera patch located on the linear deformation zone in association with an ovoid; (4) a range of volcanic features including edifices and several types of plains. Additional data (Campbell *et al.*, 1991) show that the area to the southeast of the mapped area includes additional examples of ovoids interpreted to be coronae (including a 1000 km diameter corona), tessera, plains and linear deformation belts. To a first order, these features are different from those characterizing the Ishtar Terra highlands (Sukhanov *et al.*, 1989), which suggests that the two high latitude highlands have had different geological histories.

The linear deformation belt located along the southern margin of Lavinia Planitia is one of the most distinctive features in Lada Terra. It ranges from about 250–500 km in width and is at least 6000 km in length. It trends ENE, extending toward central Lada Terra to the east outside the map area and branches northward at about 12°, 53° S extending to Alpha Regio. The southern zone consists of individual segments of generally parallel bright lineaments that range in length from 1000–1300 km. These segments are arrayed in a broad left-stepping en echelon pattern. The topography of the zone is generally characterized by a broad rise 400 km wide and ranging 0.5 to 1.0 km above the surrounding regions. Although a distinctive linear topographic trend along the strike of the lineament belt is observed, the topography is very irregular along the belt, with alternating highs and lows spaced several hundred to over a thousand km apart. In some places, these irregularities

correspond to observable features such as ovoids, tessera, volcanic source regions and edifices. In general, the linear deformation zone occurs on or close to the crest of the rise, with a spacing of lineaments in the range of 6 to 8 km (Figure 2c and 2d).

Several large circular to oval features occur along the segmented rise. In the central part of the southernmost 1000 km long en echelon segment (322.5°, 63° S), a large circular structure is observed consisting of two radar-bright concentric rings (about 185 and 280 km in diameter) (Figure 10a). The rings are defined by narrow bright linear features about 9 to 18 km apart. Some of the linear elements cut through the circular structure, while others wrap around it to form the concentric rings. A narrow zone (40–55 km wide) in the southern part of the circular structure cuts the concentricity and circularity, apparently separating the structure into two segments, in a manner similar to the separations seen in Themis Regio (Campbell *et al.*, 1991). If the structure was originally completely circular, then the separation distance of about 50 km obtained by restoring the circularity suggests that the structure has been locally extended about 18% of its diameter, compared to the 10–15% interpreted in parts of Themis. In addition, there is evidence for possible strike-slip faulting offsetting the circular structure. Apparent right-lateral offset occurs along a linear trend oriented N 65° E, offsetting both rings on both sides of the structure approximately 10 km.

The second en echelon segment (centered at 62° S, 335°, see Figure 2d), is about 1000 km long and a poorly defined oval or V-shaped structure is located near the center. The third segment (centered at 60° S, 345°) is about 1300 km long and it is interrupted just east of its mid-point by several superposed volcanic vents which are sources for the digitate flows of the Lavinia lava complex (Figure 9). In the easternmost part of this segment, the general linear trend is interrupted by more radially arrayed lineaments centered on a local topographic high (0°, 58° S; Figure 10b). Although the morphology is not clear, these structures could be related to the deformation of a volcanic edifice. At the eastern end of the third segment, the structure joins with an ovoid about 500–600 km in diameter (Figure 10b). The ovoid is bisected along an axis trending about N 40° E by bright lineaments that extend NE from a large corona feature mapped further south in Lada Terra (Campbell *et al.*, 1991). Just north of this ovoid is a patch of tessera; a linear deformation zone extends from this point for about 600 km NNW along the southern part of the 2000 km trend to Alpha Regio (Figure 2d and 2e). Further north are three structures each separated by about 600 km (Figure 10c). The central one (3°, 37° S) is similar in size and morphology to Ushas Mons, with a dark summit region and bright flanks and is interpreted to be a volcanic edifice. However, it appears to be more structurally modified than Ushas, with a hint of concentric structure, particularly to the SW and abundant evidence of radial lineaments that appear to be fractures rather than flows. Southeast of this structure (6°, 42° S) is another edifice which appears to have been structurally modified even more, with abundant evidence for concentric rings to the SW and distinctive radial

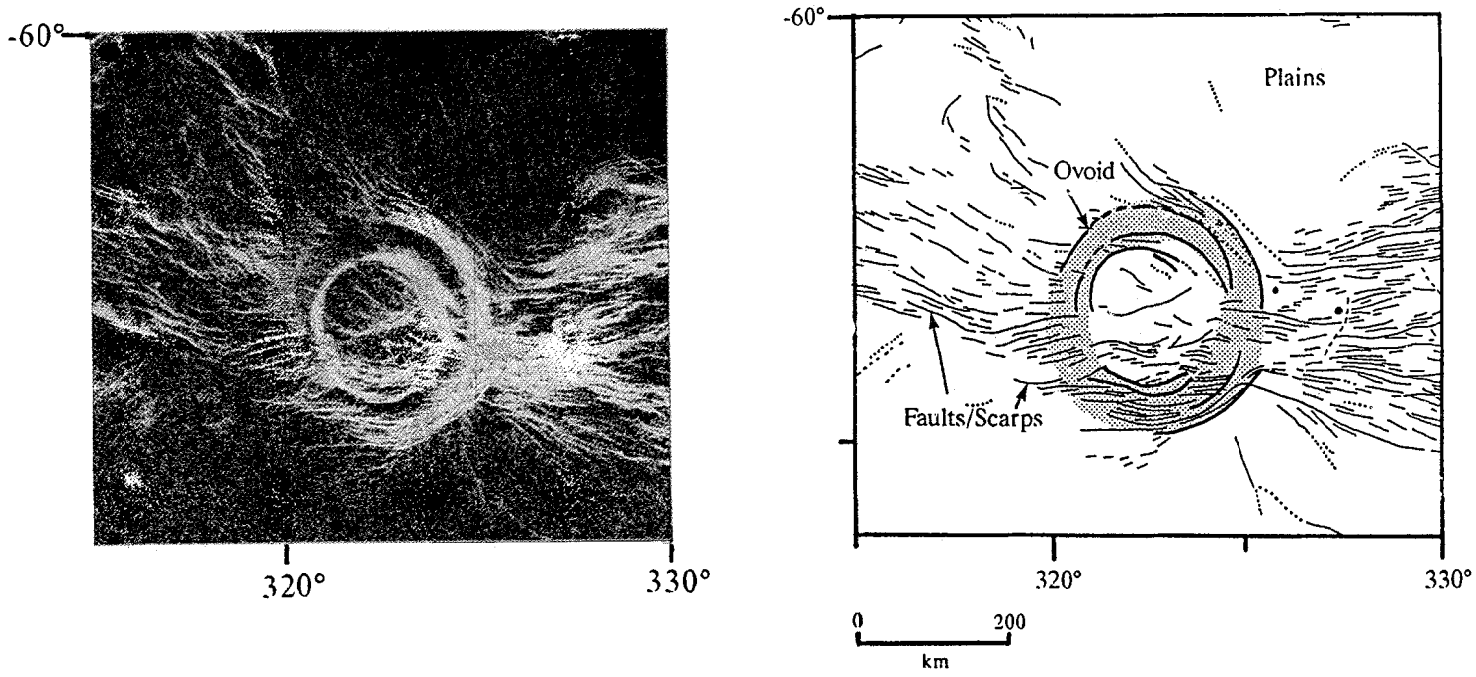

Fig. 10(a). Arecibo image and sketch map of ovoid located along the northern edge of Lada Terra. The feature both diverts and is crosscut by bright lineaments which are interpreted to be faults and scarps.

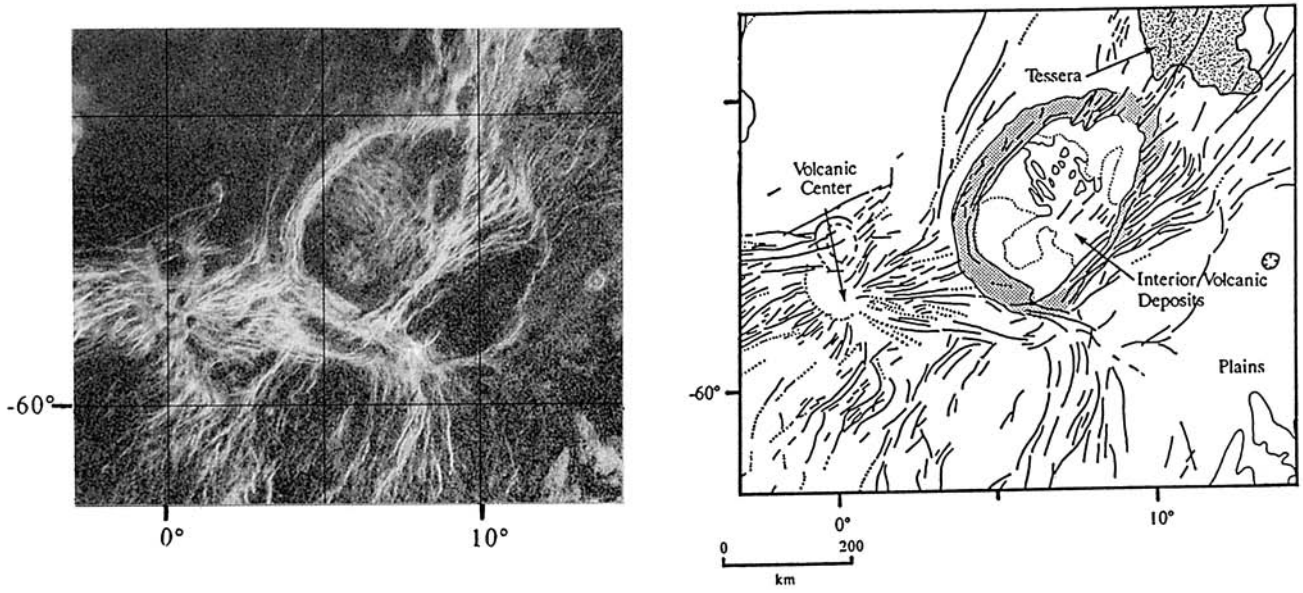

Fig. 10(b). Radar image and sketch map of ovoid and volcanic center located to the east of the lava complex. On the basis of its rim structure, presence of interior volcanic deposits and the presence of an annulus of radar-bright lineaments, this feature is interpreted to be a corona.

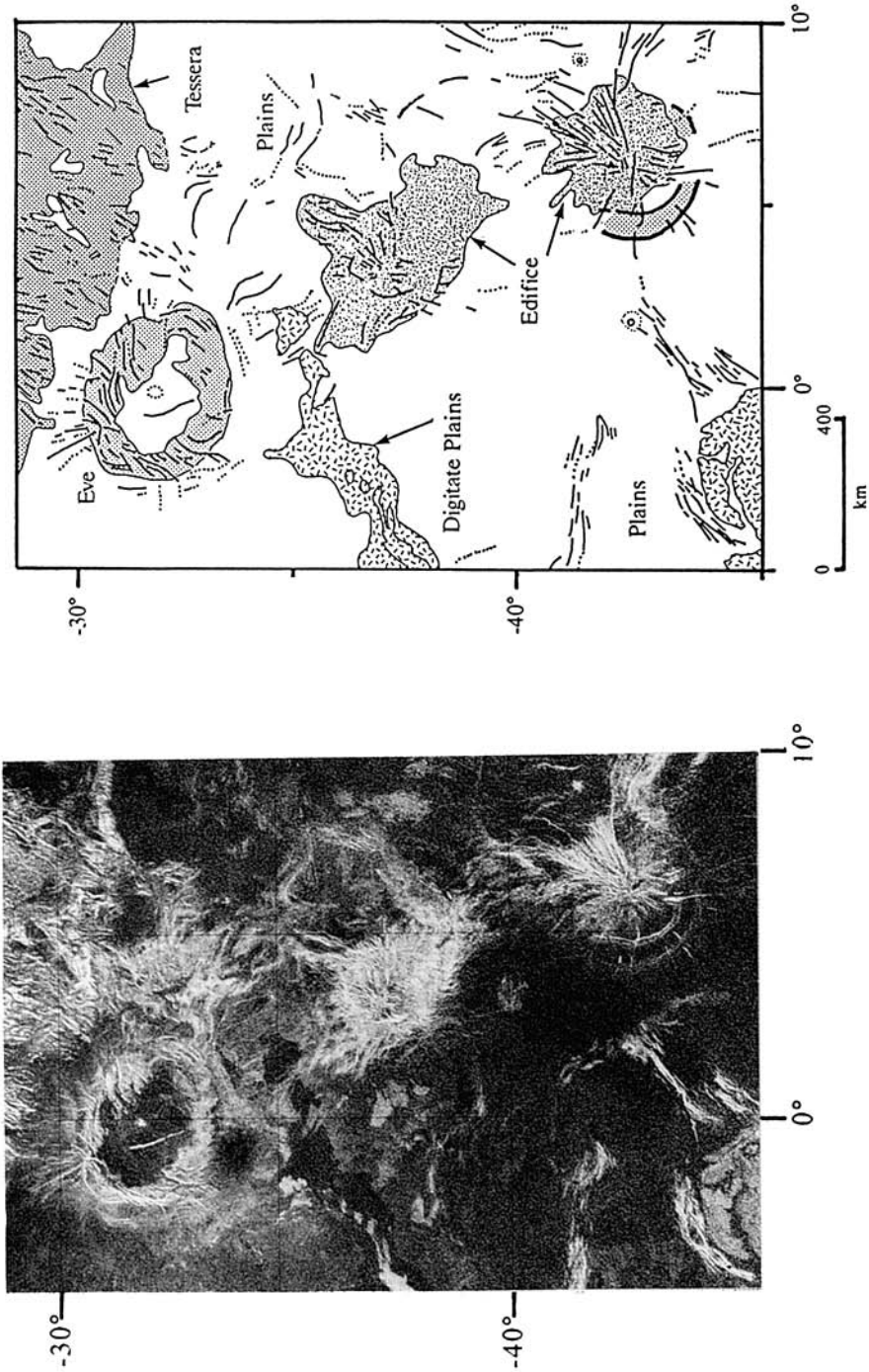

Fig. 10(c). Radar image and sketch map of an ovoid (Eve) and edifices located along a linear trend to the south and east of Alpha Regio.

texture. Northeast of the central structure is Eve, a 400–500 km diameter ovoid that does not appear to have a central edifice, but instead it has a central region of dark plains. Although there is evidence for two concentric rings (partial outer rings on the eastern and northern edges) the annulus defining Eve is raised and very heavily deformed, with structural patterns linked to regional trends in Alpha Regio (Figure 4). The appearance of these three similar sized features and comparison to Ushas Mons, suggests that there may be a sequence of formation and structural modification, with Ushas representing the generally undeformed edifice, the central structure representing the initial stages of relaxation and degradation, the SE structure representing more intense and extensive modification with development of the annulus and Eve representing the final stages, with the annulus dominating (Figure 10c). This is similar to the sequence suggested by Stofan and Head (1990; Figures 13, 15).

The large (300 × 400 km) ovoidal structure located at 7°, 57° S (Figure 10b), is very similar to features classified as coronae (Pronin and Stofan, 1990). Its elongate nature parallel to a throughgoing northeast trending lineament zone suggests that it may be deformed along this zone. The similarity in size of the concentric-ringed structure (280 km), the source region for the southern digitate flows and this ovoid and their relationship to the linear deformation zone, suggest that they may be linked in origin. The circular structure may represent surface deformation associated with initial buoyant upwelling, the digitate flows with subsequent outpouring of lavas and the ovoid with further vertical and lateral deformation.

A distinctive chevron-shaped linear deformation feature is located in the vicinity of the linear deformation zone (Figure 2e). This structure is characterized by two sets of parallel lineaments (one trending N 30° W and the other trending N 80° E) that meet at an apex which is oriented N 25° E. The linear structures are spaced 30 to 50 km apart and are generally very straight. Their morphology (ridges, troughs) cannot be determined with the available data. At the apex of the chevron, the linear features often appear to terminate and a series of irregular depressions are located there. The northern part of the apex coincides with the source region of the major occurrence of the digitate plains (Figure 2d, e). On the basis of this association, the location of arcuate and elongate features along the apex and apparent embayment relationships within the apex region, the apex is interpreted to be a volcanological source region. The spacing of the lineaments is similar to those (3 to 5 km) in other tectonic environments and cross-cutting relationships suggest that the chevron structure postdates much of the activity in the lineament belt along the northern border of Lada. The southeastern part of the chevron is generally radial to the large corona in the south (Campbell *et al.*, 1991), but the relationships of these two structures is not clear. The data presented here show that Lada Terra is made up of linear zones of deformation, ovoids and volcanic source regions. In comparison with the northern high latitude highland of Ishtar Terra which is characterized by zones of convergence and compression, this upland dominated by ovoids is interpreted to be a site of mantle upwelling.

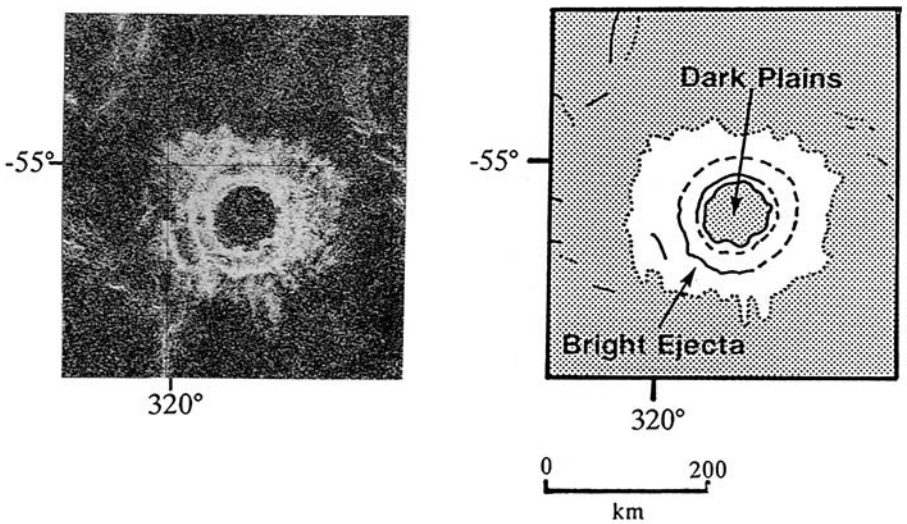

Fig. 11. Arecibo radar image and sketch map of the 157 km diameter impact basin, Lise Meitner. The dark deposits on the floor of the crater are interpreted as smooth lava deposits.

3.11. Impact craters

The characteristics of fifty-two craters mapped within the southern hemisphere (inclusive of the image data extending to 78° S) and interpreted to be of impact origin on the basis of their morphology (Campbell *et al.*, 1990; Campbell *et al.*, 1991) (Figure 2c) are listed in Table II. The smallest crater is 8 km in diameter and the largest is 157 km in diameter. Fifteen (29%) of these craters, diameters between 8 and 18 km, fall into the morphologic class of simple bowl-shaped craters. Twenty-six (50%) of these craters have central peaks, three (6%) have central peak-like rings, one (2%) (Lise Meitner) has multiple rings (Figure 11) and seven (13%) have dark (and presumably smooth) interior floors. The smallest crater with a central peak is 19 km in diameter and the largest is 66 km in diameter. Ten craters have both central peaks and dark floors. The presence of these dark deposits, interpreted as smooth lava deposits, in craters with diameters greater than 18 km suggests that they have been modified by post impact volcanism. In several cases, central peak rings are present (three craters with diameters between 43 and 59 km). Two additional craters which do not have central peak rings (50 and 66 km diameter) but have central peaks which are offset from the crater center, may contain partially flooded central peak rings.

The resolution of the image data is insufficient to determine the details of crater wall structure. The multiring structure of Lise Meitner (Figure 11) suggests that it may be similar to the crater Klinova (144 km diameter) in the northern high latitudes. The innermost ring (about 83 km diameter) is continuous and is apparently embayed along its inner base by radar dark plains similar to the plains surrounding the crater exterior deposits. No detail is seen at this resolution in the

interior plains, which we interpret to be volcanic fill. The major ring (157 km in diameter) appears distinctly scalloped along its southern border where it trends normal to the radar illumination direction. To the southwest of the crater, a bright arc is observed about 28 km from the edge of the second ring. This may represent structure associated with a partial outer ring.

Exterior deposits are visible for craters larger than about 15 km in diameter, are generally limited to about one crater radius from the rim crest and probably correspond to continuous ejecta deposits observed in other planetary craters. The morphology of exterior deposits is often radially-textured, sometimes petal-like and often asymmetric. In some cases, one or two narrow sinuous lobate flow-like bright deposits extend up to several crater radii beyond the rim. Of the thirty-eight craters greater than 15 km in diameter, twenty-two (58%) show evidence of asymmetry in their exterior or ejecta deposits. Of these, half are characterized by diffuse ejecta and the rest by bright ejecta. The orientation of these deposits shows a generally random distribution, with some apparent enhancement in the south and southwest directions. At Lise Meitner, exterior to the 157 km diameter ring, are lobate petal-like features interpreted to be bright deposits of ejecta, similar to many of the lobes seen in smaller craters. The largest extends about 60 km from the second ring. The different patterns of ejecta emplacement suggests that these deposits may have been heavily modified by post-impact processes such as volcanism, or that their mode of emplacement is more complex than on airless planets (Schultz and Gault, 1979).

The technique of crater counting is typically used to determine stratigraphic relations and ages of different geologic units on planetary surfaces. The lack of a significant number of craters on the individual units mapped in the southern hemisphere does not allow this technique to be used here; however, it is possible to use the density and size/frequency distribution of craters to estimate a general age for the portion of the surface imaged by Arecibo (Campbell *et al.*, 1990). Within the 55.6×10^6 km^2 imaged, the density craters per 10^6 km^2 is found to 0.94. In comparison with other parts of the planet, imaged at a comparable resolution, this value is less than the 1.56 craters per 10^6 km^2 estimated for the northern high latitudes from Venera 15/16 data (45° N to the north pole) (Basilevsky *et al.*, 1987) and similar to the 0.89 craters per 10^6 km^2 calculated for the equatorial region (1° S to 45° N) and suggests an age for the surface comparable to the 0.3 billion to 1.0 billion year age determined for these areas (Ivanov, 1986; Basilevsky *et al.*, 1987; Schaber *et al.*, 1987).

4. Summary, Comparison to Other Areas and Conclusions

An analysis of Arecibo radar images shows the southern hemisphere of Venus to be characterized by diverse styles of tectonism and volcanism. In this section, we: (1) compare the distribution of geologic units with those mapped on other parts of the planet, (2) summarize the major geologic processes thought to be occurring

in the southern hemisphere and (3) identify a number of problems to be addressed from higher resolution MAGELLAN data.

The units mapped in the Venus southern hemisphere can be divided into two groups, those that are primarily volcanic and those that are tectonic. Volcanic units include plains (inclusive of all subtypes), edifices and ovoids (those not associated with the ovoid chain) while tectonic units are made up of tessera, linear deformation zones and the ovoid chain. Plains are the most abundant unit in the southern hemisphere comprising 78% of the area imaged, slightly greater than the 71% of the surface in the northern high latitudes imaged by Venera 15/16 (Bindschadler and Head, 1989) and similar to the 80% for the portion of the equatorial region imaged by Arecibo (Senske *et al.*, 1991), indicating that volcanism forming plains is a globally significant process. Edifices are found to make up about 3% of the surface in the southern hemisphere, a percentage comparable to that in the equatorial region. This unit is similar to regions mapped from Venera data as large dome-like uplifts (areas including edifices and their surrounding rises, e.g. Beta Regio and Bell Regio) which make up 2.6% of the northern high latitudes. In this study we mapped only the individual edifices; if we include rises such as the one on which Ushas, Innini and Hathor Montes are located, then these features are found to make up a percentage slightly greater than 3%. Ovoids make up only 0.4% of the surface, similar to the equatorial region, but significantly less than the 2.9% mapped from Venera images. If the large coronae in the southern part of Lada Terra (Campbell *et al.*, 1991) are also included, outside the area mapped, then ovoids are found to make up 4% of the southern hemisphere. Tessera, the most abundant tectonic unit in the northern high latitudes (14%), makes up only a small percentage of the southern latitudes (3%), with the greatest concentration of tessera located at Alpha Regio. This significant difference suggests that the process forming tessera may be less dominant in the southern high latitudes. The most abundant tectonic unit in the region imaged by Arecibo are linear deformation zones (12%). In comparison to similar features elsewhere on the planet (ridge belts and furrow belts; 7.6% of northern high latitudes), these zones make up a higher percentage of surface area, indicating that this form of deformation is more abundant in the southern high latitudes, or that its surface expression is more readily preserved in this region. The unit that has no apparent counterpart elsewhere on the planet is the ovoid chain. This unit makes up 4% of the mapped area and extends toward Atla Regio at the western boundary of the image. Additional analysis of other data sets, Pioneer Venus topography, roughness and reflectivity, suggests that the lateral extent of this unit is greater than that observed in the Arecibo images.

A number of formational mechanisms are proposed for features mapped in the Venus southern hemisphere. On the basis of embayment relations, presence of lobate flows and compositional analysis of surface material from Venera landers, plains are interpreted to be volcanic in origin. The styles of volcanism within the plains ranges from constructional, forming domes and edifices, to lava flooding,

resulting in the emplacement of high volumes of extremely fluid lavas. Volcanic deposits on the rise containing Ushas, Innini and Hathor Montes are interpreted to contribute only a small part to the broad regional topography of this area. On the basis of evidence for limited and localized volcanism, broad domal topography, the convergence of tectonic zones forming relations similar to areas in the equatorial region interpreted to be associated with mantle upwelling and the presence of plains on the high topography similar to those in the surrounding lowlands, this region is interpreted to be associated with mantle upwelling resulting in the uplift of plains and volcanism building edifices. Ovoids and the ovoid chain are similar to coronae and on this basis are interpreted to have formed in association with hotspots. The presence of apparent split and separated ovoids in Themis Regio, suggests that extension as well as mantle upwelling has occurred. Formational models proposed for these and other features in the southern hemisphere suggest that mantle upwelling or hotspots on a number of scales may be an important mechanism of lithospheric heat transfer for this part of Venus.

Zones of linear deformation form an interconnecting network extending from the west at the edge of the image coverage to the east through Themis Regio, connecting with Hathor Mons and continuing southwest to Lada Terra where it branches in an east-west direction (Figure 2d). These relations along with analysis of other parts of the planet (Senske, 1990) suggest that zones of tectonism mapped in the southern hemisphere are part of a more widespread system of interconnecting tectonic zones. It is observed that at least one tectonic zone mapped in the equatorial region extends into the southern hemisphere. The rift valley, Devana Chasma, extends south from the tectonic junction of Beta Regio cuts across Phoebe Regio, with lineaments splaying to form a pattern along the southern part of Phoebe much like that observed at the northern part of Beta (Stofan *et al.*, 1989). The collection of lineament belts in Lavinia Planitia form a pattern similar to ridge belts adjacent to Atalanta Planitia. On the basis on their local elevation, location in a broad topographic low, the lack of split and separated features and their similarity to ridge belts in the northern high latitudes interpreted to be compressional, linear deformation zones in Lavinia Planitia are interpreted to be primarily of compressional origin. On the basis of the analysis of the image data, two conclusions can be reached regarding tectonism on Venus: (1) assuming that all the tectonic features, e.g. linear deformation zones, are presently active, then Venus is characterized by a tectonic style in which stresses are distributed over great distances resulting in widespread deformation over distances of 1000's of km; (2) assuming that many of the tectonic features observed are no longer active, but preserved due to low rates of erosion, then tectonism and stresses are concentrated along relatively narrow zones of deformation (along zones 100's of km wide).

Arecibo imaging of the Venus southern hemisphere has revealed the broad regional geologic character of this part of the planet and has provided a basis to propose mechanisms of formation for a variety of features. We conclude our

analysis by identifying a number of problems that can be addressed from higher resolution MAGELLAN data.

The tessera of Alpha Regio is shown to be characterized by multiple episodes of deformation, but is nearly completely surrounded by undeformed plains. Additional data should provide insight as to how this region initially formed, allow the development of a stratigraphic history for the various episodes of deformation and facilitate an analysis to determine its relation to the series of ovoids and edifices extending to the southeast from Eve. The highland containing Ushas, Innini and Hathor Montes is interpreted to be associated with a region of mantle upwelling; additional data will help determine the relative contributions of constructional volcanism and dynamic support of topography and may provide evidence of an age relation between the volcanoes. A number of ovoids making up the ovoid chain at Themis Regio are observed to be interbeaded, MAGELLAN images should provide a basis to better determine cross cutting and age relations between the various structures, allowing an assessment of the various formational models presented here. In most cases it is not possible to determine if linear deformation zones are composed of faults, scarps, or ridges, additional higher resolution images should make these relations clear. Finally, the lowland of Lavinia Planitia is a basin, additional data will help to assess if this region has subsided with resulting deformation causing the formation of lineament belts, much like the lunar maria.

Acknowledgements

The research presented in this report was supported by NASA grants from the Planetary Astronomy and Geology and Geophysics programs of NASA's Office of Space Science and Applications (DBC), NAGW-2185 (JWH) and a National Academy of Sciences–National Research Council Associateship (ERS). Portions of this analysis were carried out when one of the authors (DAS) was a graduate student research fellow at Goddard Spaceflight Center (NTG-50147). Helpful discussions with R. Vorder Bruegge, D. Bindschadler, A. T. Basilevsky, E. N. Slyuta, V. Kryuchkov and G. A. Burba are gratefully acknowledged. The Arecibo Observatory is part of the National Astronomy Ionosphere Center which is operated by Cornell University under a cooperative agreement with the National Science Foundation and with support from NASA.

References

ACSN: 1961, 'Code of Stratigraphic Nomenclature', *Am. Assoc. Petroleum Geologists Bull.* **45**(5), 645–660.

Aubele, J. C.: 1990, 'Arecibo-Venera Comparison of Domes in Guinevere Planitia', Venus (abstract), *Lunar Planet Sci. Conf.* **XXI**, 30–31.

Aubele, J. C. and Slyuta, E. N.: 1990, 'Small Domes on Venus: Characteristics and Origin', *Earth, Moon and Planets*, **50/51**, 493–532.

Barsukov, V. L., Basilevsky, A. T., Burba, G. A., Bobina, N. N., Kryuchkov, V. P., Kuzmin, R.

O., Nikolaeva, O. V., Pronin, A. A., Ronca, L. B., Chernaya, I. M., Shashkina, V. P., Garanin, A. V., Kushky, E. R., Markov, M. S., Sukhanov, A. L., Kotelnikov, V. A., Rzhiga, O. N., Petrov, G. M., Alexandrov, Y. N., Sidorenko, A. I., Bogomolov, A. F., Skrypnik, G. I., Bergman, M. Y., Kudrin, L. V., Bokshtein, I. M., Kronrod, M. A., Chochia, P. A., Tyuflin, Y. S., Kadnichansky, S. A., and Akim, E. L.: 1987, 'The Geology and Geomorphology of the Venus Surface as Revealed by the Radar Images Obtained by Veneras 15 and 16', *J. Geophys. Res.*, **91**, D378–D398.

Basilevsky, A. T., Pronin, A. A., Ronca, L. B., Kryuchkov, V. P., Sukhanov, A. L., and Markov, M. S.: 1986, 'Styles of Tectonic Deformations on Venus: Analysis of Venera 15 and 16 Data', *J. Geophys. Res.* **91**, D399–D411.

Basilevsky, A. T., Ivanov, B. A., Burba, G. A., Chernaya, I. M., Kryuchkov, V. P., Nikolaeva, O. V., Campbell, D. B., and Ronca, L. B.: 1987, 'Impact Craters of Venus: A Continuation of the Analysis of Data from the Venera 15 and 16 Spacecraft', *J. Geophys. Res.* **92**, B12, 12869–12901.

Bindschadler, D. L. and Head, J. W.: 1988, 'Diffuse Scattering of Radar on the Surface of Venus: Origin and Implications for the Distribution of Soils', *Earth, Moon and Planets*', **42**, 133–149.

Bindschadler, D. L. and Head, J. W.: 1989, 'Characterization of Venera 15/16 Geologic Units from Pioneer Venus Reflectivity and Roughness Data', *Icarus* **77**, 3–20.

Bindschadler, D. L. and Head, J. W.: 1991, 'Tessera Terrain, Venus: Characterization and Models for Origin and Evolution', *J. Geophys. Res.* **96**, 5889–5907.

Bindschadler, D. L., Kreslavsky, M. A., Ivanov, M. A., Head, J. W., Basilevsky, A. T., and Shkuratov, Yu. G.: 1990, 'Distribution of Tessera Terrain on Venus: Predictions for MAGELLAN', *Geophys. Res. Lett.* **17**, 171–174.

Campbell, D. B. and Burns, B. A.: 1980, 'Earth-Based Radar Imagery of Venus', *J. Geophys. Res.* **85**, 8271–8281.

Campbell, D. B., Head, J. W., Harmon, J. K., and Hine, A. A.: 1984, 'Venus: Volcanism and Rift Formation in Beta Regio', *Science* **226**, 167–170.

Campbell, D. B., Head, J. W., Hine, A. A., Harmon, J. K., Senske, D. A., and Fisher, P. C.: 1989, 'Styles of Volcanism on Venus: New Arecibo High Resolution Data', *Science* **246**, 373–377.

Campbell, D. B., Stacy, N. J. S., and Hine, A. A.: 1990, 'Venus: Crater Distribution at Low Northern Latitudes and in the Southern Hemisphere from New Arecibo Observations', *Geophys. Res. Lett.* **17**, 1389–1392.

Campbell, D. B., Senske, D. A., Head, J. W., Hine, A. A., and Fisher, P. C.: 1991, 'Venus Southern Hemisphere: Geologic Characteristics and Age of Major Terrains in the Themis-Alpha-Lada Region', *Science* **251**, 180–183.

Esposito, P. B., Sjogren, W. L., Mottinger, N. A., Bills, B. G., and Abbott, E.: 1982, 'Venus Gravity: Analysis of Beta Regio', *Icarus* **51**, 448–459.

Evans, J. V. and Hagfors, T.: 1964, 'On the Interpretation of Radar Reflections from the Moon', *Icarus* **3**, 151–160.

Farr, T. G. and Anderson, R. S.: 1987, 'Simulation of Surface Modification Processes in Arid Regions: Applications to Remote Sensing and the Study of Climate Change', *Geol. Soc. Amer. Abstracts with Program* **19**, 659.

Ford J. P.: 1980, 'Seasat Orbital Radar Imagery for Geologic Mapping: Tennessee–Kentucky–Virginia', *Amer. Assoc. of Petroleum Geologists Bull.* **64**, 2064–2094.

Frank, S. L. and Head, J. W.: 1990a, 'Styles of Compressional Deformation on Venus: Examples from Ridge Belts (abstract)', *Lunar and Planet. Sci.* **XXI**, 387–388.

Frank, S. L. and Head, J. W.: 1990b, 'Ridge Belts on Venus: Morphology and Origin', *Earth, Moon and Planets* **50/51**, 421–470.

Goldstein, R. M., Green, R. R., and Rumsey, H. C.: 1976, 'Venus Radar Images', *J. Geophys. Res.* **81**, 4807–4817.

Greeley, R. and Martel, L.: 1988, 'Radar Observations of Basaltic Lava Flows, Craters-of-the-Moon, Idaho', *Int. J. Remote Sensing* **9**, 1071–1085.

Head, J. W.: 1990, 'Venus Trough-and-Ridge Tessera: Analog to Earth Oceanic Crust Formed at Spreading Centers', *J. Geophys. Res.* **95**, 7119–7132.

Head, J. W. Adams, J. B.: McCord, T. B., Pieters, C., and Zisk, S.: 1978, 'Regional Stratigraphy and Geologic History of Mare Crisium, in Mare Crisium: The View from Luna 24', R. B. Merrill and J. J. Papipke (Eds.), Pergamon Press, New York, pp. 43–47.

Head, J. W. and Crumpler, L. S.: 1987, 'Evidence for Divergent Plate-Boundary Characteristics and Crustal Spreading on Venus', *Science* **238**, 1380–1385.

Head, J. W. and Wilson, L.: 1986, 'Volcanic Processes and Landforms on Venus: Theory, Predictions, and Observations', *J. Geophys. Res.* **91**, B9, 9407–9446.

Head, J. W., Peterfreund, A. R., and Garvin, J. B.: 1985, 'Surface Characteristics of Venus Derived from Pioneer Venus Altimetry, Roughness, and Reflectivity Measurements', *J. Geophys. Res.* **90**, 6873–6885.

Ivanov, B. A., Basilevsky, A. T., Kryuchkov, V. P., and Chernaya, I. M.: 1986, 'Impact Craters of Venus: Analysis of Venera 15 and 16 data', *J. Geophys. Res.*, **91**, B4, D413–D430.

Janle, P., Jannsen, D., and Basilevsky, A. T.: 1987, 'Morphologic and Gravimetric Investigation of Bell and Eisila Regiones on Venus', *Earth, Moon and Planets* **39**, 251–273.

Keddie, S. T., Head, J. W., and Campbell, D. B.: 1990. 'Volcanic Centers in Northern Lavinia Planitia (abstract)', *Lunar Planet. Sci. Conf.* **XXI**, 615–616.

Kryuchkov, V. P. and Basilevsky, A. T.: 1989, 'Radar-Bright Flow-Like Features as Possible Traces of the Latest Volcanic Activity on Venus (abstract)', *Lunar Planet. Sci. Conf.* **XX**, 548–549.

Kryuchkov, V. P.: 1989, 'A System of Conjugate Strike-Slip Faults in the Ridge Belts of Venus (abstract)', *Lunar Planet. Sci. Conf.* **XX**, 546–547.

Masursky, H., Eliason, E., Ford, P. G., McGill, G. E., Pettengill, G. H., Schaber, G. G., and Schubert, G.: 1980, 'Pioneer-Venus Radar Results: Geology from Images and Altimetry, *J. Geophys. Res.* **85**, 8232–8260.

MacDonald, H. C.: 1980, 'Techniques and Applications of Imaging Radar', in B. S. Siegel and A. R. Gillespie (Eds.), *Remote Sensing in Geology*, Chapter 10, John Wiley and Sons, New York.

McGill, G. E., Steenstrup, S. J., Barton, C., and Ford, P. G.: 1981, 'Continental Rifting and the Origin of Beta Regio', *Geophys. Res. Letters* **6**, 739–742.

McGill, G. E., Warner, J. L., Malin, M. C., Arvidson, R. E., Eliason, E., Nozette, S. N., and Reasenberg, R. D.: 1983. 'Topography, Surface Properties and Tectonic Evolution, in D. Hunten, M. L. Colin, T. M. Donahue, and V. I. Moroz (Eds.), *Venus*, University of Ariz. Press, pp. 69–130.

Morgan, P. and Phillips, R. J.: 1983, 'Hot Spot Heat Transfer: Its Application to Venus and Implications to Venus and Earth', *J. Geophys. Res.* **88**, B10, 8305–8317.

Nikishin, A.: 1986, 'Hotspot Tectonics on Venus: Implications for Rifting and Doming (abstract)', *Lunar Planet Sci. Conf.* **XVII**, 615–616.

Pettengill, G. H., Eliason, E., Ford, P. G., Loriot, G. B., Masursky, H., and McGill, G. E.: 1980, 'Pioneer Venus Radar Results: Altimetry and Surface Properties', *J. Geophys. Res.* **85**, 8261–8270.

Phillips, R. J., Kaula, W. M., McGill, G. E., and Malin, M. C.: 1981, 'Tectonics and Evolution of Venus', *Science* **212**, 879–887.

Pieters, C. M., Head, J. W., Adams, J. B., McCord, T. B., Zisk, S. H., and Whitford-Stark, J. L.: 1980, 'Late High-Titanium Basalts of the Western Maria: Geology of the Flamsteed Region of Oceanus Procellarum', *J. Geophys. Res.* **85**, 3913–3938.

Pronin, A. A., Sukhanov, A. L., Tyuflin, Yu. S., Kadnichanskij, S. A., Kotelnikov, V. A., Rzhiga, O. N., Petrov, G. I., Sidorenko, A. I., Alexandrov, Yu. N., Krivtsov, A. P., Sinho, V. P., Burba, G. A., and Bobina, N. N.: 1986, 'Geological-Morphological Description of the Lakshmi Planum (Photomap of the Venusian Surface Sheet B-4)', *Astron. Vestnik*, **20**, 83–98.

Pronin, A. A. and Stofan, E. R.: 1990, 'Coronae on Venus: Morphology, Classification and Distribution', *Icarus* **87**, 452–474.

Raitala, R. and Tormanen, T.: 1989, 'Coronae Chain on Venus – A Hotspot Structure under a Moving Plate?' (abstract), *Lunar Planet. Sci. Conf.* **XX**, 882–883.

Reasenberg, R. D., Goldberg, Z. M., MacNeil, P. E., and Shapiro, I. I.: 1981, 'Venus Gravity: A High Resolution Map', *J. Geophys. Res.* **86**, 7173–7179.

Roberts, K. M and Head, J. W.: 1990, 'Lakshmi Planum, Venus: Characteristics and Models of Origin', *Earth, Moon and Planets* **50/51**, 193–249.

Saunders, R. S. and Mutch, T. A.: 1980, 'Extraterrestrial Geology, in B. S. Siegel and A. R. Gillespie (Eds.), *Remote Sensing in Geology*, Chapter 20, John Wiley and Sons, New York.

Saunders, R. S., Pettengill, G. H., Arvidson, R. E., Sjogren, W. L., Johnson, W. T. K., and Pieri, L.: 1990, 'The MAGELLAN Venus Radar Mapping Mission', *J. Geophys. Res.* **95**, 8339–8355.

Schaber, G. G.: 1982, 'Venus: Limited Extension and Volcanism Along Zones of Lithospheric Weakness', *Geophys. Res. Lett.* **9**, 499–502.

Schaber, G. G.: 1988, 'Elevations of Venusian Shields as Indicators of Lithospheric Thickness (abstract)', *Lunar Planet Sci. Conf.* **XIX**, 1023–1024.

Schaber, G. G.: 1990, 'Volcanism on Venus as Inferred from the Morphology of Large Shields', *Proceedings of the 22nd Lunar and Planetary Science Conference*, in press.

Schaber, G. G. and Kozak, R. C.: 1989, 'Morphologies of Ten Venusian Shields Between Lat 30° and 90° N. (abstract)', *Lunar Planet. Sci. Conf.* **XX**, 954–955.

Schaber, G. G., Shoemaker, E. M., and Kozak, R. C.: 1987, 'The Surface of Venus: Use of the Terrestrial Cratering Record, *Astron. Vestnik*, **21**, 144.

Schultz P. H. and Gault, D. E.: 1979, 'Atmospheric Effects on Martian Ejecta Emplacement', *J. Geophys. Res.* **84**, 7669–7687.

Senske, D. A.: 1990, 'Geology of the Venus Equatorial Region from Pioneer Venus Radar Imaging', *Earth, Moon and Planets* **50/51**, 305–327.

Senske, D. A. and Head, J. W.: 1989, 'Venus Equatorial Geologic Units (abstract)', *Lunar Planet. Sci. Conf.* **XX**, 986–987.

Senske, D. A., Campbell, D. B., Stofan, E. R., Fisher, P. C., Head, J. W., Stacy, N., Aubele, J. C., Hine, A. A., and Harmon, J. K.: 1991, 'Geology and Tectonics of the Beta Regio, Guinevere Planitia and Western Eistla Regio, Venus: Results from High-Resolution Arecibo Image Data', this issue *Earth, Moon and Planets* **55**, 163–214.

Slyuta, E. N.: 1990, 'Large Shield Volcanoes (>100 km in Diameter) on Venus: Morphologic Types (abstract)', *Lunar Planet Sci. Conf.* **XXI**, 1172–1173.

Slyuta, E. N., Nikolaeva, O. V., and Kreslavsky, M. A.: 1988, 'Distribution of Small Domes on Venus: Venera 15/16 Radar Data', *Solar System Res.* **22**, 8295–8302.

Slyuta, E. N. and Kreslavsky, M. A.: 1990, 'Intermediate (20–100 km) Sized Volcanic Edifices on Venus (abstract)', *Lunar Planet Sci. Conf.* **XXI**, 1174–1175.

Solomon, S. C. and Head, J. W.: 1990, 'Lithospheric Flexure Beneath the Freyja Montes Foredeep Venus: Constraints on Lithospheric Thermal Gradient and Heat Flow', *Geophys. Res. Lett.* **17**, 1393–1396.

Stofan, E. R. and Head, J. W.: 1990, 'Coronae of Mnemosyne Regio: Morphology and Origin', *Icarus* **83**, 216–243.

Stofan, E. R., Head, J. W., and Campbell, D. B.: 1985, 'Multiple Ring Features in Themis Regio: Evidence for Endogenic Origin (abstract)', *Lunar. Planet. Sci. Conf.* **XVI**, 824–825.

Stofan, E. R., Head, J. W., and Campbell, D. B.: 1987, 'Geology of the Southern Ishtar Terra/ Guinevere and Sedna Planitiae Region on Venus', *Earth, Moon and Planets* **38**, 183–207.

Stofan, E. R., Head, J. W., Campbell, D. B., Zisk, S. H., Bogomolov, A. F., Rzhiga, O. N., Basilevsky, A. T., and Armand, A.: 1989, 'Geology of a Rift Zone: Beta Regio and Devana Chasma', *Geol. Soc. Am. Bulletin*, **101**, 143–156.

Stofan, E. R., Head, J. W., and Campbell, D. B.: 1990a, 'Beta-Eistla Deformation Zone: Analysis from Recent Arecibo Images (abstract)', *Lunar. Planet. Sci. Conf.* **XXI**, 1208–1209.

Stofan, E. R., Head, J. W., and Campbell, D. B.: 1990b, 'Themis Regio, Venus: Analysis from High Resolution Arecibo Images (abstract)', *Lunar. Planet. Sci. Conf.* **XXI**, 1210–1211.

Sukhanov, A. L., Pronin, A. A., Burba, G. A., Nikishin, A. M., Kryuchkov, V. P., Basilevsky, A. T., Markov, M. S., Kuzmin, R. O., Bobina, N. N., Shashkina, V. P., Slyuta, E. N., and Chernaya, I. M.: 1989, 'Geomorphic/Geologic Map of Part of the Northern Hemisphere of Venus', *U.S. Geol. Surv. Misc. Invest. Ser. Map I–2059.*

Sukhanov, A. L. and Pronin, A. A.: 1989, 'Ridged Belts on Venus as Extensional Features', *Proceedings of the 19th Lunar and Planetary Science Conference*, Lunar and Planetary Institute, Houston, pp. 335–348.

Watters T. R.: 1988, 'Wrinkle Ridge Assemblages on the Terrestrial Planets', *J. Geophys. Res.* **93**, 10,236–10,254.

Wilhelms, D. E.: 1970, 'Summary of Lunar Stratigraphy – Telescopic Observations', *U.S.G.S. Prof. Paper 599-F, F1–F47.*

Wilhelms, D. E.: 1972, 'Geologic Mapping of the Second Planet, *USGS Interagency Report: Astrogeology* **55**, 36 p.

Wilson, L. and Head, J. W.: 1988, 'Nature of Local Magma Storage Zones and Geometry of Conduit Systems below Basaltic Eruption Sites: Pu'u O'o, Kilauea East Rift, Hawaii, Example, *J. Geophys. Res.*, **93**, B12, 14,785–14,792.

Zuber, M. T.: 1987, 'Constraints on the Lithospheric Structure of Venus from Mechanical Models and Tectonic Surface Features', *J. Geophys. Res.* **92**, E541–E551.

Zuber, M. T. and Parmentier, E. M.: 1990, 'On the Relationship between Isostatic Elevation and the Wavelengths of Tectonic Surface Features on Venus', *Icarus*, **85**, 290–308.